Romanian Journal of Earth Sciences, vol. 89, issues 1-2, p. 1-33

The magmatic immiscibility between silicate-, brine-, and Fe-S-O melts from the porphyry (Cu-Au-Mo) deposits in the Carpathians (Romania): a review

Ioan PINTEA*

Geological Institute of Romania (IGR), Cluj Napoca branch

Abstract: The magmatic fluid phase immiscibility between salt-, silicate-, and Fe-S-O melts from Miocene porphyry Cu-Au-(Mo) deposits from Metaliferi Mountains and Eastern Carpathians in Romania is characterized based on ultrahigh temperature microthermometry (i.e. ≥ 900°-1100°C) and petrography of the fluid and melt inclusions assemblages, and was described first time two decades ago by the author, mainly in the potassic zone from some of these ore deposits, i.e. Deva, Roşia-Poieni, Tarnita, Bolcana, Rovina, Valea-Morii, Tălagiu in Metaliferi Mountains and Suplai-Măgura Neagră from Ţibles massif in Eastern Carpathians. These data are reviewed here and new data and interpretations are added. There are five major types of fluid and melt inclusions in the investigated deposits (i.e. silicate melt, hydrous salt melt, vapor-rich, aqueous liquid-rich and globular (Fe-S-O) immiscible melt). The magmatic immiscibility between silicate-salt-(Fe-S-O) melt at ≥ 900°-1100°C and calculated pressure range from 0.3 and 12.8 kbars was documented in separate and/or coeval inclusions. Two main processes were involved in their generation: (1) direct exsolution from magma and (2) endogeneous autometasomatism. These processes started deep in the magma source and finished in the upper levels of the shallow intrusives in complex stratovolcanoes and/or calderas.

***Keywords*:** hydrous salt melt, silicate melt, Fe-S-O melt, vapor-rich, aqueous liquid-rich, inclusion assemblages, petrography, microthermometry, immiscibility, porphyry copper deposit

1. Introduction

There are at least 14 known porphyry copper occurrences in the Metaliferi Mountains, Romania (Milu et al., 2004). The immiscibility between silicate melt and hydrous salt melt in these deposits from Metaliferi Mountains (Romania) was documented firstly in quartz by petrographic and microthermometric studies (Pintea, 1993, 1995, 1996, 1997). The silicate melt, hydrous salt melt and aqueous fluid inclusions are also coexistent with globular sulfide inclusions in magmatic-hydrothermal quartz in these deposits, so we can describe in reality immiscibility between silicate-saline-(Fe-S-O) melts and aqueous fluid phases (Pintea, 2002, 2009). The microthermometry shows that these processes took place first at very high P-T conditions (≥ 900°-1100°C and 0.3-12.8 kbars) characterizing the endogenous stage of the magmatic-to-hydrothermal systems of the main porphyry copper occurrences of Miocene mineralized intrusions in the area, i.e. Deva, Roşia-Poieni, Tarniţa, Bolcana, Rovina, Valea-Morii and Tălagiu in Metaliferi Mountains, and also in Măgura Neagră-Suplai zone from Ţibles massif in Eastern Carpathians (Pintea, 1996; Pintea et al., 1999a). Anyhow, many questions still remained, such as whether the immiscible phases were involved in the ore formation in these deposits, or perhaps they are conspicuous products of the complex magmatic-hydrothermal processes, including autometasomatism (Pintea, 2010). It is very probable that the salt melt was exsolved first, as homogeneous salt globules during the primary and secondary boiling processes (Burnham, 1979), and overprinted by fluid/melt-rock interaction in the brittle/ductile stress conditions or mafic magma mingling-mixing (e.g. Cloos, 2001). We assume that these processes produced multiple fluid and melt inclusions assemblages during quartz

* email:ipinteaflincs@yahoo.com

crystallization from the hydrosilicate-rich phases. In the mean time, it should be stressed that an exolved fluid phase of about 10 wt% NaCl split during the magmatic-to-hydrothermal transition (Burnham, 1979) in pairs of low density fluid phase and high salinity liquid containing up to 70 wt% NaCl, trapped in coeval inclusions (Bodnar et al., 1985). That is the consequence of the large immiscibility field in NaCl-H_2O system where vapor and liquid phases are coexistent (Cline and Bodnar, 1991; Heinrich, 2007; Bodnar, 2010). A superposition of the above mentioned processes can be documented sometimes in the same sample, in time-sequences of fluid inclusion generations (assemblages), but obviously was very difficult to find the exact pair of the fluid phases as snapshot of the fluid phase separation event(s). Nevertheless, there is a great progress now in the fluid phase equilibrium analysis by a new generation of analytical tools, theoretical and computer-software facilities (e.g. Harris et al., 2003; Heinrich et al., 2005; Driesner and Heinrich, 2007; Webster and Mandeville, 2007; Bodnar, 1995; 2010). The ore elements were complexed mainly as chlorides and precipitated from the hydrous salt melt as sulfides and oxides, depending on the initial S content and oxygen fugacity, which is in the range of magnetite-hematite buffer (Burnham and Ohmoto, 1980, Eugster, 1986). The increase of water content after its saturation in the silicate melt by the first and secondary boiling processes would change drastically the molten salt chemistry by more successive episodes of boiling and dilution. The (Fe-S-O) immiscible melts were also released as the main result of an autometamorphic process driven by the final magma crystallization at relatively ultrahigh P-T conditions (≥900° - 1100°C, 0.3 - 12.8 kbars), emphasized by Pintea (2010). The hydrothermal processes would be complicated even more by the addition of meteoric water, which would create a medium to low P-T (≤ 650°C, 0.5-1 kbar) convective system centered on the protore zone and surroundings, enhancing the economic ore concentrations in veins and breccias by alteration processes (Pintea, 1996, and unpublished reports).

Fluid inclusion evidence of immiscibility at high P-T conditions between silicate melt and saline rich fluids in porphyry copper deposits (PCDs) and others silicate rocks was documented by many authors worldwide, and high homogenization temperatures of the brine inclusions were reported by Ryabchikov, (1963), Roedder and Coombs (1967), Roedder (1970, 1981, 1984, 1992), Reyf and Bazeyev (1977), Wilson et al. (1980), Eastoe and Eadington (1986), Solovova et al. (1991), Frezzotti (1992), Pintea (1993, 1995, 1997), Lowenstern (1994), Yang and Bodnar, (1994), Reyf (1997), Campos et al. (2002), Kamenetsky et al. (2004), Fulignati et al. (2001, 2005), Kamenetsky (2006), Davidson and Kamenetsky (2007), Kamenetsky and Kamenetsky (2010), Li et al. (2011), Kodera et al. (2012, 2014). Magmatic immiscibility between silicate melt, salt melt and Fe-Cu sulfide melt was identified and described by Pintea (2002, and unpublished report) in the Upper Cretaceous porphyry Cu-Mo deposits from South Carpathian in Banat. Fluid-salt-melt evolution and the sources of fluids from high pressure magma chamber were described at Banská - Štiavnica magmatic-hydrothermal system in Western Carpathians (Naumov et al., 1996). Fluid-melt immiscibility in various P-T-X conditions was documented during experimental works related to chloride, silicate, sulfide, sulphate, borate fluids, e.g., Koster van Groos and Wyllie (1969), Shinohara et al. (1989), Ballhaus et al. (1994), Thomas et al. (2000), Martel and Bureau (2001), Veksler et al. (2002), Antignano and Manning (2008) and many others.

In this research, the author presents the most important petrographic and microthermometric data related to fluid and melt inclusions study "as they are" in a cluster of porphyry Cu-Au(Mo) deposits occurring in the Metaliferi Mountains (South Apuseni Mountains) and Magura Neagră-Suplai from Ţibleş massif, which is situated in the Eastern Carpathians subvolcanic zone. Somehow, these data seem to make up an uncommon data set, suggesting very high P-T trapping conditions. These could be probably related to the specific geodynamics of the Eastern Carpathians and Apuseni Mountains during middle Miocene. A strong argument is based upon the published geothermometry (802° - 1416°C) and geobarometry (3.2 - 9.7 kbars) of the minerals formed from the magmatic processes originated in the mantle wedge above subducted slab in the Eastern Carpathians (e.g. Kovacs, 2002). The magmas and associated ore deposits from the Apuseni Mountains were formed during the middle Miocene extension (or post collision evolution of a metasomatized mantle lithosphere under astenospheric upwelling) related to the decompression melting

in a high thermal regime (Roşu et al., 2004; Seghedi et al. 2010; Harris et al., 2013). High temperature up to 1000°C was suggested in the processes associated with subduction and postsubduction geotectonic settings worldwide (Richards, 2003, 2009; Li et al., 2011). Moreover, it was documented, at global scale, that the W-directed subduction processes, evolved in a very high thermal regime (Doglioni et al., 2009). The subduction in the Carpathians was W-directed, as mentioned by Seghedi et al. (2004).

Another explanation for these uncommon high T-P trapping conditions for the silicate and hydrous salt melt inclusions, probably more likely, could be related to the specific post-entrapment modifications or heterogeneous trapping mechanism, as suggested in the literature (e.g. Hall and Sterner, 1993; Li et al., 2009; Bodnar, 2003; Kamenetski and Danyusevski, 2005; Lerchbaumer and Audetat, 2012; and references therein).

2. Geological setting

The basement of Metaliferi Mountains from South Apuseni Mountains in Romania consists of complex Palaeozoic metamorphic rocks, Mesozoic ophiolites and sedimentary deposit, Upper Cretaceous-Paleogene and pre-Badenian magmatites and Miocene sedimentary deposits. The porphyry deposits are of Cu-Au(Mo)-types and clustered in the conventionally named "gold quadrilateral"(Ghiţulescu and Socolescu, 1941), associated or overprinted by low and high sulphidation epithermal Au-rich mineralization mainly with Au-tellurides, which mark the anomalous richness of Au in the area and also the enrichment of Cu (Fig. 1). The gold is known and exploited from immemorial times but real scientific investigations on the mineralogy, metallogeny and mining geology related to the epithermal and, later, on the porphyry copper mineralization were documented by Ghiţulescu and Socolescu (1941), Ianovici et al. (1977), Berbeleac (1985, 1988), Mitchell and Carlile (1994), Mârza (1999), Udubaşa et al. (2001), Vlad and Orlandea (2004), Seghedi et al. (2004), Roşu et al. (2004); Neubauer et al. (2005), and many others. The porphyry copper system described in the Ţibleş massif situated in the Eastern Carpathians, specifically in the subvolcanic zone, shows many petrological and geochemical features typical for a porphyry copper deposit (Udubaşa et al., 1983, Pintea et al., 1999a). Their fluid and melt inclusions microthermometry and petrography are comparable with those described in the Metaliferi Mountains, but the geological setting is different and still under debate (Udubaşa et al., 1984).

The host rock of the PCDs in the Metaliferi Mountains consisted of amphibole-, and biotite-andesite to quartz dioritic and microdioritic rocks in complex subvolcanic structures (Boştinescu, 1984; Berbeleac et al., 1995, Udubaşa et al., 2001). As a rule, in the stratovolcano edifice (or calderas) the latest intruded shallow body has been Cu-Au mineralized and the volcanic activity is a prerequisite in the development of the intrusions, these frequently being intruded at the bottom of the eruption cone. The main alteration products are related to the potassic, phyllic, propylitic and argillic facies and mineralization is typical of porphyry Cu-Au (Mo) described by Ianovici et al. (1977), Vlad (1983), Boştinescu (1984), Udubaşa et al. (2001), Roşu et al. (2001), Milu et al. (2004), Ivăşcanu, et al.(2003), Kouzmanov et al.(2005, 2006), among others. Typical quartz veins networks occur in all potassic zones of these deposits and host melt and fluid inclusions assemblages of various types (Fig. 2). Alternatively and/or complementary, the mineral assemblages from these deposits (Pintea, 2010) and similar ones worldwide could be formed as magmatic driven endogen (autometamorphic) products during the formation of the high temperature potassic and phyllic zones (Harris and Golding, 2002; Seedorff et al., 2005; Cathles and Shanon, 2007; Wilkinson and Cooke, 2011) (Fig. 3). The main mineralogical parageneses of the veinlets include quartz-bornite, quartz-magnetite, quartz – chalcopyrite - magnetite, quartz-pyrite, anhydrite-pyrite, etc. Quartz is present as small prismatic or doubly-terminated crystals occurring in some breccia zones.

The characteristic small veins have a coarse-grained texture and frequently form complicated cross-cutting systems with different ages and composition (Fig. 3, Fig 4). See also Damman et al. (1996), Milu (2004), Heinrich (2007), Kouzmanov et al., (2010) and references therein, for the complex relationships of veinlets cross-cutting.

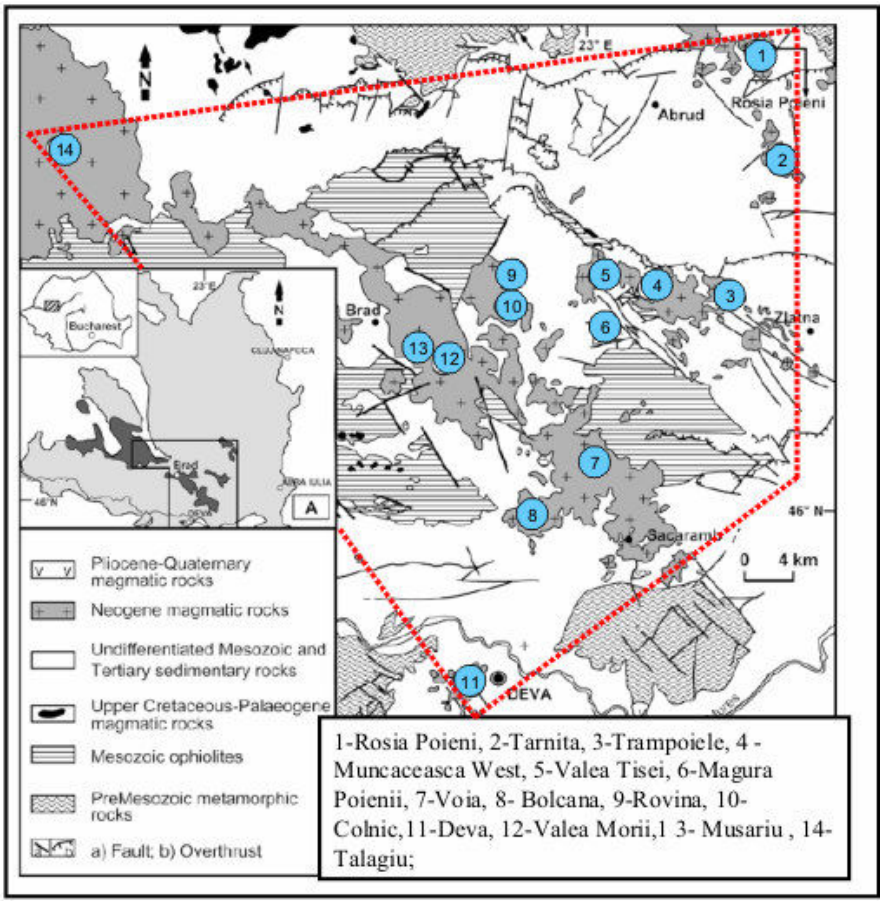

Fig.1. Cluster of Miocene porphyry Cu-Au-(Mo) deposits in the "Gold Quadrilateral" from Metaliferi Mountains (South Apuseni Mountains region - modified from Milu et al., 2004).

3. Methods

3.1. Sample collection and preparation.

The quartz samples were collected from outcrops, drill cores and from underground mines and open pits, specifically for each porphyry copper deposit. Generally they were separated from the characteristic vein networks from potassic zone, including breccia clasts by hammer crushing; then, doubly polished thin sections (e.g. Fig. 3) were prepared from faceted quartz crystals (3-15 mm length), or from quartz grains (1 to 5mm in size), and these were observed under the petrographic microscope. Totally, at least 100 thin polished sections (including wafers) were studied from the most representative quartz samples and used for petrography and microthermometry, as summarized in Table 1A.

3.2. Microthermometry

The micro-thermometric experiments were done in a Linkam TS 1500 stage installed and calibrated by the author in the Institute of Mineralogy and Petrography at ETH Zurich (as "akademicher gast", 1994). The system was adapted under a Leitz petrographic microscope equipped with a L32 (UTK 50) lens. For calibration, the melting points of $K_2Cr_2O_7$ (398°C), NaCl (801°C) and Au (1064°C) were used. For temperature higher than 200°C a correction value was added to the thermocouple readings using a calibration curve. The accuracy of recorded temperature ranged between 10° and 15°C for temperatures above 800°C.

The microthermometry was completed with additional measurements in a personal "home made device" used only between 20° up to 1100°C (Pintea, 1998- unpublished report). The heating procedure was selected as a function of the melt inclusion type. For silicate melt inclusion high heating and cooling rates 5° to 20°C/min and 50° to 100°C/min were used, respectively. For salt melt inclusions were recorded more than three melting points, and the heating rate was carefully selected. Consequently, around the melting point of each solid phase, the temperature was held for several

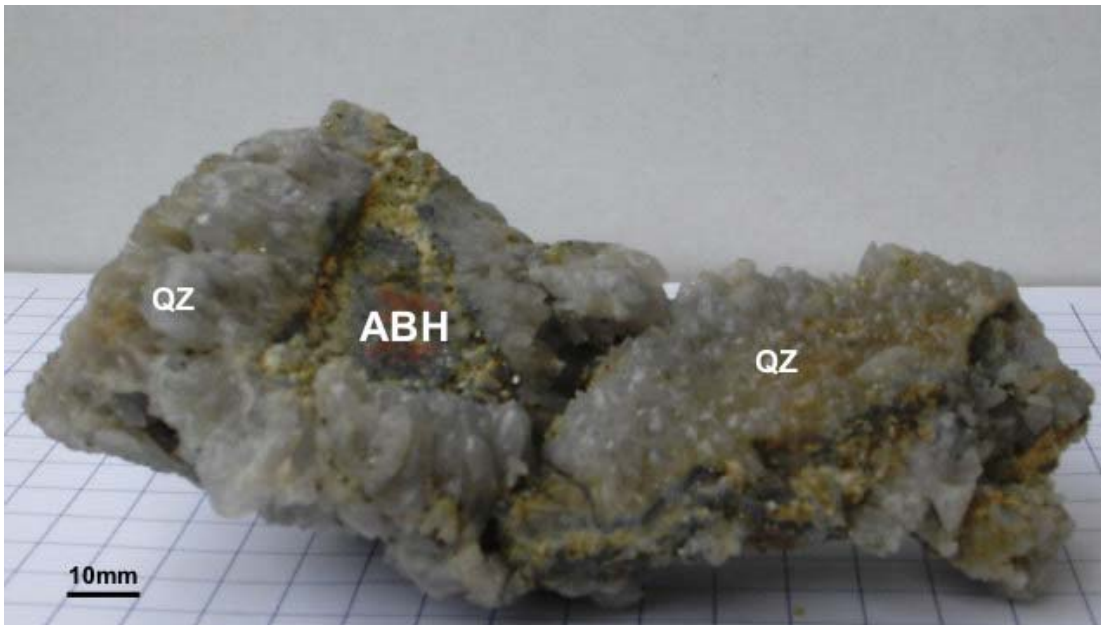

Fig. 2. Large prismatic quartz phenocrysts(QZ) from the potassic zone from the Rosia Poieni Cu-Au(Mo) deposit. An angular fragment of altered andesite (ABH) is covered by precipitated quartz crystals from a brecciated zone inside the deposit. They contains unique high temperature brine and vapor-rich inclusions assemblages related to multiple growth zones as depicted in Fig. 4.

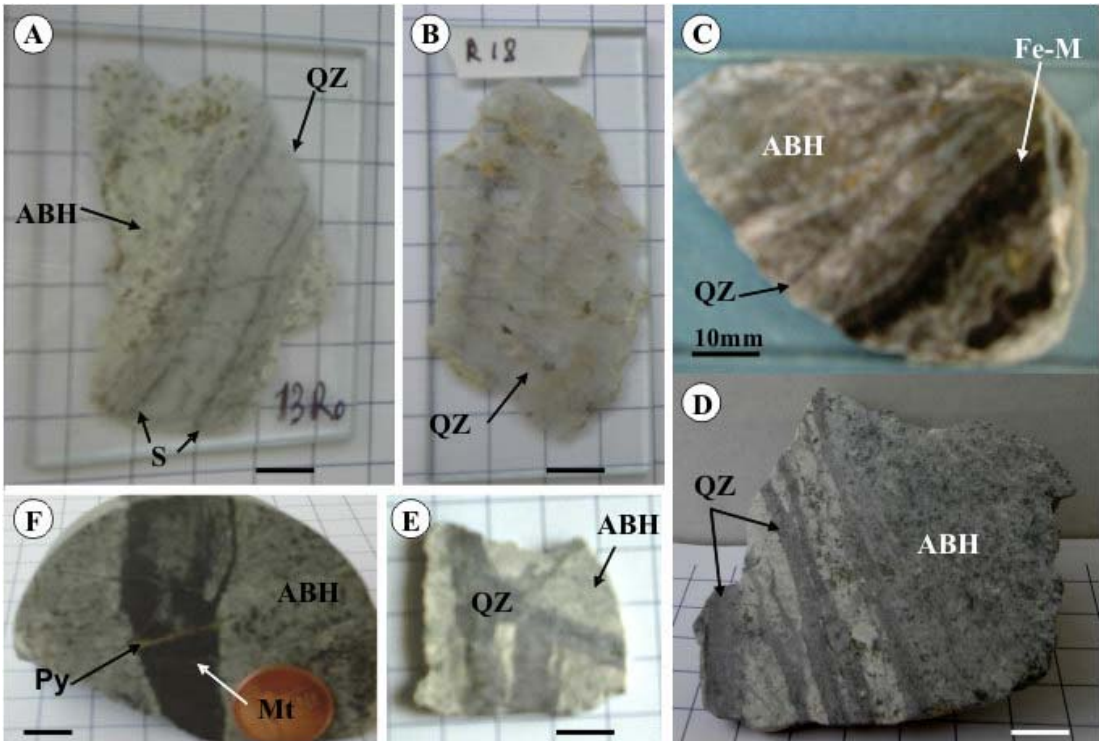

Fig. 3. Quartz vein sample as double polished thin sections (**A**- Rovina, **B**- Rosia Poieni) formed by coarse grain quartz and very thin veinlets with sulfide in a intense altered biotite-, and hornblende- andesite (ABH); **C**- Double polished thin section from Valea Morii PCD showing an alternate of quartz grain veinlets with altered andesite (ABH) and another Fe- rich metasomatic assemblage(Fe-M); **D**. Hand specimen of altered andesite (ABH) intersected by parallel multiple quartz veinlets; E. polished surface of a hand specimen with quartz veinlet intersection in altered andesite at Talagiu; **F**- magnetite (Mt) veinlets in the potassic zone from Bolcana PCD crosscut by late pyrite (Py) veinlet. Scale bar = 10 mm.

Table 1A. Summarized characteristics of the quartz samples showing immiscibility evidence between silicate-, salt-, and (Fe-S-O) melts from the porphyry copper system from Metaliferi Mountains and Ţibles massif.

Ore deposit	Sample type	Location/alteration	Inclusion types	Distribution	Immiscibility-evidence type
Deva	quartz grains, faceted crystals (2-3mm)	veinlets, breccia potassic phyllic	slicate glass hydrous salt melt ±aqueous liquid	random, in growth zones cluster, trails	a, b,c
Roşia Poieni	quartz grains. faceted crystals up to 15mm	veinlets, druzes potassic phyllic	silicate glass ± aq liquid; hydrous salt melt	trails in growth zones cluster	a, b, c
Tarniţa	quartz grains	veinlets potassic phyllic	silicate glass hydrous salt melt	trails cluster	a, b, c
Bolcana	quartz grains	veinlets (magnetite-rich) potassic phyllic	silicate melt hydrous salt melt	in growth zones trail cluster	a, b, c
Rovina	quartz grains; faceted quartz crystals (2-3mm)	veinlets potassic	silicate glass hydrous salt melt	trail cluster	a, c
Valea Morii	quartz grains; faceted quartz crystals (2-5mm)	veinlets potassic phyllic	silicate glass hydrous salt melt	in growth zones trails cluster	a, b, c
Tălagiu	quartz grains	veinlets potassic phyllic propylitic	silicate melt silicate glass hydrous salt melt	in growth zones cluster trail	a, b, c
Ţibleş massif	quartz grains	veinlets aplites potassic phyllic propylitic	silicate silicate melt hydrous salt melt	cluster trail	a, b, c

Abbreviations: a-singular inclusion containing silicate glass + hydrosilicate melt; b-Coeval silicate melt or silicate glass with hydrosilicate melt; c-silicate melt released around salt melt±vapor during the microthermometric runs.

Table 1B. EPMA analyses of the silicate melt inclusions associated with hydrous salt melt in quartz veins from the potassic zone from Deva porphyry copper deposit (Pintea, 1995).

Compound	P1	P2	P3	P4	P5	P6	P7
SiO_2	71.57	72.61	73.86	74.02	76.21	76.86	72.55
Al_2O_3	16.01	16.92	16.40	11.82	14.18	10.83	15.89
FeO	0.26	0.40	0.35	0.29	0.41	0.27	0.45
MnO	0.03	0.03	0.02	0.05	0.00	0.00	0.09
MgO	0.04	0.01	0.04	0.00	0.04	0.03	0.03
CaO	0.26	0.30	0.21	0.35	0.21	0.13	0.28
Na_2O	2.06	1.83	1.96	1.37	1.55	1.46	2.31
K2O	4.98	3.88	5.34	3.50	4.00	3.49	5.01
Cl	0.35	0.36	0.34	0.28	0.23	0.19	0.34
Total	95.47	96.25	96.37	91.45	96.76	93.22	96.86
F,Cl=O	0.08	0.08	0.08	0.06	0.05	0.04	0.08
Total	95.40	96.17	96.29	91.39	96.71	93.18	96.78

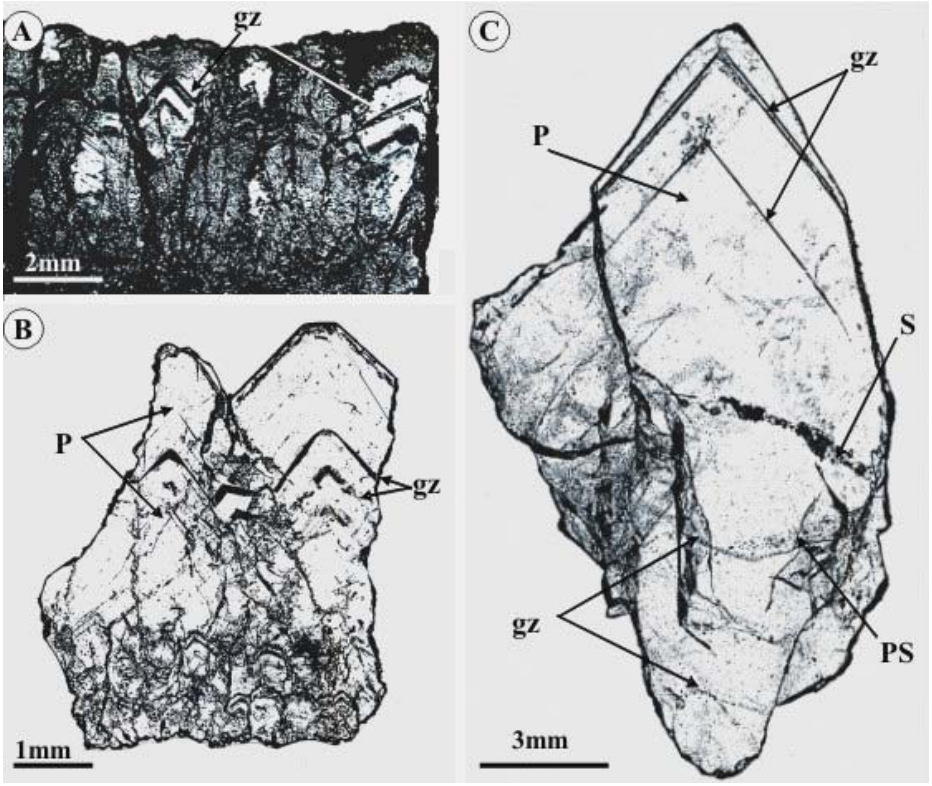

Fig. 4. Transversal sections in quartz grain veinlets (A, B) and monocrystaline-zoned quartz individual showing the distribution of silicate, saline, vapor rich and sulfide/oxide inclusions in Deva (A, B) and Rosia Poieni (C). All inclusions could be Primary (P), Pseudosecondary (PS) and secondary decorating growth zones(gz), cicatrized plain fissures as trails

minutes and the heating rate ranged between 5° and 10°C. Close to the melting or homogenization temperature a lower rate was used ranging between 2° and 5°C.

The duration of one complete run took sometimes several hours depending on the inclusion type; for brine inclusions, 30 to 50 minutes were enough to be heated up and then cooled down to room temperature. More than 500 microthermometric measurements were made especially on the hydrous salt-, and silicate melt inclusions. Because of the complex chemical composition and difficulty on the identification of the solid daughter phases the salinity was approximated only from halite melting points. To estimate salinity in w% NaCl eq the program SoWat[1] was used (Driesner and Heinrich, 2007), and all old data estimation for salinity were updated by using this software. The highest values are representative for the hydrous salt melt inclusions, in which, at high temperature, the chloride liquid coexists with a silicate rich melt.

3.3. EPMA analyses

The glassy part of silicate melt inclusion brought onto the surface by polishing before the microthermometric experiments (only glass + small vapor bubble). Analyses were performed using a CAMECA SX-50 electron microprobe at the Institut für Mineralogie und Petrographie, ETH Zürich (Pintea, 1995). The microprobe is equipped with five crystal spectrometers and operated at an acceleration potential of 15 kV and a beam current of 10 nA on a Faraday cage, and a "spot" size of 1μ. Samples and standards were coated with 200Å of carbon. Glasses shown constant compositions (Table 1B) close to a normal granite, being similar with other chemical data for salt-silicate immiscibility documented in several granites worldwide by Reyf and Bazheyev, (1977); Harris, (1986); Frezzotti, (1992), or in the experimental study by Shinohara et al., (1989), Webster, (1997a), and many others.

[1] SoWat program was built-up by T. Driesner at ETH- Institute of Geochemistry and Petrology (Swiss) and SoWat stands for Sodium chloride-Water and is a model (almost an equation of state) for the properties of fluids in the H_2O-NaCl system. See the references list at the end of this paper.

3.4. Supplementary techniques.

During the last two decades the author used, in collaboration with different researchers, several complementary analytical method such as SEM/EDS (Damman et al., 1996, Pintea, 1996), crush-leach technique for the bulk chemical analyses (Pintea, 1998, unpublished report), chlorine isotopic ratio (Pintea et al., 1999b), gas extraction by coupled GC-MS technique (Cună et al., 2001). All of these data are not the subject of this review but some of them were mentioned when necessary.

4. Fluid inclusion petrography

At room temperature conditions several types of melt and fluid inclusions were described, mainly based upon the mode of occurrence and the number and nature of trapped phases, as follows: - *Silicate melt inclusions* (crystallized melt +/-glass +/- vapor bubble(s) +/- immiscible droplet of chloride rich fluid);
- *Silicate glass inclusions* (mainly glass + vapor bubble (s) +/- chloride rich fluid or only glass);
- *Hydrous salt melt inclusions* (multiple daughter phases such as chlorides, sulphates, sulphides/oxide +/- silicate+ vapor bubble);
- *Vapor - rich inclusions* (vapor mainly +/- liquid +/- solids);
- *Aqueous liquid - rich fluid inclusions* (liquid dominant +/- a vapor bubble);
- *Globular sulfide/oxide melt inclusions* (Fe-S-O) opaque globular solid phases.

In between, we can recognize various combinations where the ratios among solid, liquid and vapor phases are in any proportion as a result of heterogeneous trapping. All of the mentioned types of inclusions are primary, pseudosecondary (trapped generally as trails in recicatrized microcracks formed during the growth of the host mineral) and secondary, based upon phase relation, shape and distribution related to quartz microtexture. They are mono-, bi-, and multiphase fluid and melt inclusions occording to the phase number at room temperature conditions. Because there are frequent growths zones and trails in the magmatic-hydrothermal quartz crystals or in quartz grains, a clear distinction between different temporal genetic types of fluid and melt inclusions was documented (e. g. Fig. 4).

4.1 Silicate melt inclusions. Silicate melt inclusions are characteristic of the quartz crystals which occur in short vein networks or in complex mineralogical association including pyrite, bornite, chalcopyrite, magnetite in some breccia pipe bodies, for example at Deva porphyry Cu-Au (Mo) deposit (Boştinescu, 1983, unpubl report). It is necessary to note here that silicate glass remnants with or without other entrapped phases such as brine or vapor were described in all porphyry copper system from Metaliferi Mountains and they are characteristic not only for the high temperature processes but also for relatively low temperature hydrothermal events. Silicate glass remnants were found also as microinclusions in the opaque minerals by SEM/EDS (Nedelcu et al., 2003). Various in shape and size, this kind of inclusions occur as typical associations in crystal growth zones (Fig. 3, Fig. 5). Multiple growth zones can be recognized even in the single small crystal (1-3 mm), suggesting successive growing stages, but the PTX- conditions seem to be similar, according to Burnham's retreating-downward crystallization model (Burnham, 1979), which postulated that under the saturated carapace, the system is recovering its characteristics for each new explosive events, until extinct. As a result, it is apparent that the shallow body looks like a singular intrusion which shows precise PVTX-characteristics (Becker, 2008; Bodnar, 2010), but at the mineral scale, only the internal microtexture can reveal the real sequence of such complex processes. In other words, each small quartz veinlet is a micro-picture of the entire system. Cumulated, they composed the central stockwork, as the mineralized core of the porphyry copper system. The autometasomatic and remelting features complicated much more the picture and frequently is very difficult to say if the silicate glass inclusions are magmatic or metasomatic-hydrothermal product. Anyway, the magmatic silicate glass inclusions occur as isolated clusters or decorating the growth zone of the host mineral (Fig 5). The metasomatic-hydrothermal silicate glass inclusions occur mainly in healed microfissures, suggesting pseudosecondary and secondary origin. At room temperature conditions, they contain silicate glass and variable amounts (5-10% vol.) of globular saline phase. The glass phase is optically isotropic and colorless, and, during the microthermometric experiments up to 500°-600°C, no visible phase transition has been observed. In addition, the criteria enounced by Anderson (1991), concerning the hourglass inclusions and their magmatic significance, were also taken into account. However, in our case, they contain variable proportions of a chloride-rich phase and, consequently, the simple glass

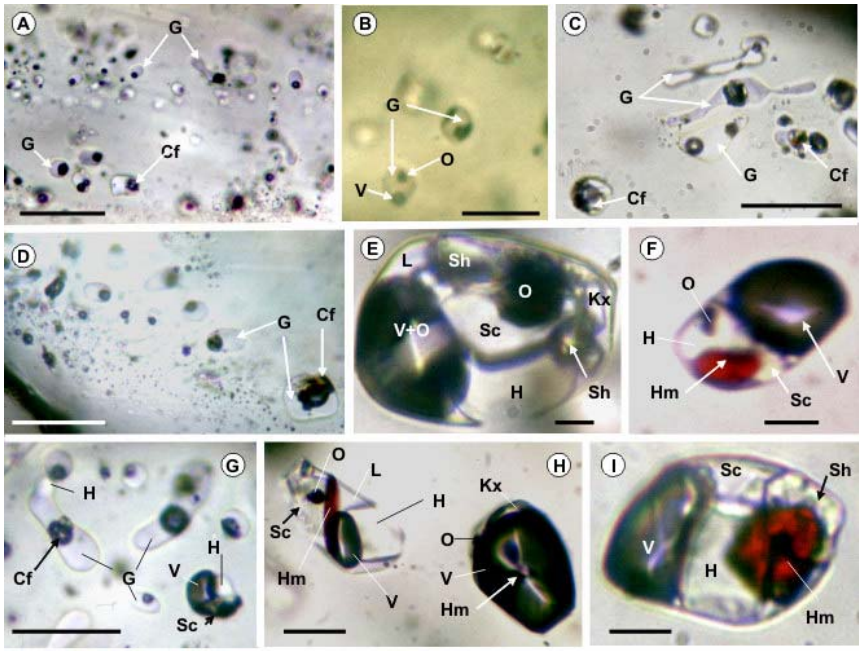

Fig. 5. Microphotographs showing several kind of silicate glass inclusions, vapor-rich and hydrous salt melt inclusions in quartz from Deva (A, C, D, E, F,G, I) and Rosia Poieni (B,H) porphyry copper systems. G-glass, Cf-saline fluid, H-halite, V-vapor, Sc- another salt daughter phase, Hm-hematite, Kx- unidentified solid phases, Sh- probable anhydrite, O-opaques - pyrite, magnetite, bornite etc; Scale bar = 20 microns.

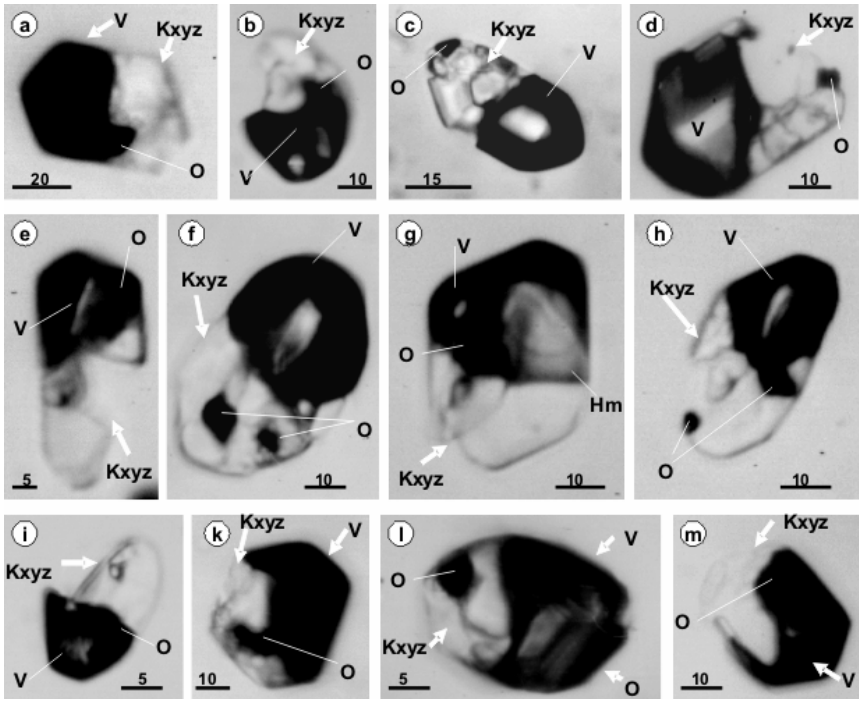

Fig. 6. Liquid - free hydrous salt melt - type inclusions at room temperature conditions from Deva Porphyry Cu-Au(Mo).Notations: Kxyz-multiple "daughter" salt microcrystals including halite,V- vapor, O-opaque. Scale bar in microns

plus vapor bubble inclusions, typical in many volcanic phenocrysts (Clocchiatti, 1975; Roedder, 1984), were difficult to be recognized in our studied samples.

This variable volumetric ratio between silicate melt and saline rich fluids in silicate glass inclusions is the result of heterogeneous trapping (Roedder, 1992). The initial mixture is formed by the silicate liquid and an exsolved chloride during magmatic to hydrothermal conditions (Fig. 5). Consequently, the fluid mixture is a sample of the growing medium from the potassic zone, where the quartz crystals occur together with K-feldspar, biotite, amphibole and some metallic minerals such as pyrite, bornite, chalcopyrite, magnetite and hematite being a product of crystallization and not the initial fluid exsolved from the magma. The "hourglass" like shape of many of these inclusions suggest a decompression process supported by the high viscosity silicate-rich phase (the direct result is expressed by the unusual shape of the cavities) during explosive release episodes (brecciation processes, too), generating the multiple growth zones in the quartz crystals. Another explanation for the variable amount of chloride melt in the

silicate melt inclusion can be the necking-down after trapping in the recicatrized microcracks. More features of this type of melt inclusions are the following:
- occasionally, in the decorated growth zones of quartz, silicate melt and/or salt melt occur, having constant proportion between the enclosed phases;
- at room temperature, the "chloride" side of these melt inclusions is a mixture of salt crystals and some silicate/sulphate rich phases (K-feldspar, anhydrite plus silicate glass identified by SEM/EDS analyses, see Fig 8 below); they are representative for the heterogeneous trapping, when variable quantities of chloride melt were exsolved from the silicate melt and enclosed in the same cavities;
- the frequent association with a "pure" fused salt inclusion, which, in turn, is primary and even pseudosecondary or secondary, suggests that the quantity of exsolved chloride melt was quite different, depending on various factors such as decreasing pressure-temperature conditions, or the fluid- rock interaction during autometasomatism;
- the quartz and fluid inclusion microtexture suggested that the evolution of the fluid phase proceeded by the separation of more and more chloride rich fluid, as the silicate magma crystallized, and by simultaneously and successive autometasomatic reactions between fluids and crystallizing minerals;
- a liquid H_2O-rich inclusion, mono-, or multiphase, is related to the remelting microtextures, in which a lot of globular Fe-rich (sulfide/oxide/silicate) phases can be recognized as a result of the autometasomatic processes. The monophasic liquid inclusions occur in characteristic associations in the quartz grains and probably are representative for the decompression process as it was described in volcanic environments and in the experimental run products (e.g. Martel and Bureau, 2001). In the mean time, the missing vapor bubble in the "superheated" aqueous fluids could be the consequence of metastability, also experimentally documented (Shmulovich et al., 2009). It is worth to emphasize that a H_2S phase could be released during these processes and perhaps this could be involved in the high sulfidation process overprinting the potassic and phyllic zones, for example at Roşia Poieni porphyry Cu-Mo(Au) deposit (Pintea, 2012).
- a special attention is required now to the presence of the globular silicate glass of hydrosilicate gel or silicothermal fluid (Wilkinson et al., 1996) formed in the magmatic-to-hydrothermal conditions, ripened and then solidified (crystallized) as saccharoidal and comb quartz microtextures encountered as the very common quartz veinlets network in porphyry copper systems worldwide (e..g. Muntean and Einaudi, 2000; Harris et al., 2004; Vasyukova et al., 2008; Pintea, 2010; Vasyukova, 2011).

The chemical composition of the amphibole andesite, the rock type hosting the PCDs from Metaliferi Mountains, shows broad variation ranges of SiO_2 (57 - 63%), K_2O (0.8 - 1.9%) and Al_2O_3 (9 - 20%), as shown, for example, by Boştinescu (1984). In comparison, the chemical composition of the glass in the silicate melt inclusions from Deva PCD showed higher SiO_2 and K_2O contents and lower concentrations of MnO, MgO and CaO (Table 1 B). A preliminary conclusion is that the most part of the metallic elements were partitioned as chloride compounds in saline rich phase before being trapped in the quartz crystals as inclusions, thus the silicate melt enclosed is just a residual hydrosilicate including aqueous saline fluids, vapor and sulfide globules. It is worth noting that the chlorine content ranges between 0.14 to 0.36 %, according to our measurements, which is in agreement with the majority of chlorine content values measured on natural specimens and in experimental works, where immiscibility between silicate and hydrous salt melt was described (e.g. Metrich and Rutherford, 1992; Webster, 1997b; Shinohara, 1994; Signorelli and Carroll, 2000). Melt inclusions trapped in plagioclase phenocrysts from mineralized versus barren intrusion were used to characterize the calc-alkaline magmas associated with Valea - Morii PCD from Metaliferi Mountains (Grancea et al., 2001). Nevertheless, it is necessary to notice that there is not yet enough analytical data on all generation-types of silicate glass inclusions associated with brine, vapor-rich and sulfide/oxide minerals to give a complete petrological conclusion for the silicate melt trapped in the minerals from the porphyry copper systems of the Metaliferi Mountains and Ţibleş massif. There are also overprinted magmatic-autometasomatic stage(s) on mafic and felsic minerals that released large quantity of hydrosilicate phase containing salt-, (Fe-S-O)-melts and aqueous fluids globules, which decorated the old and new minerals phantom-microtextures (Pintea, 2010). The presence and

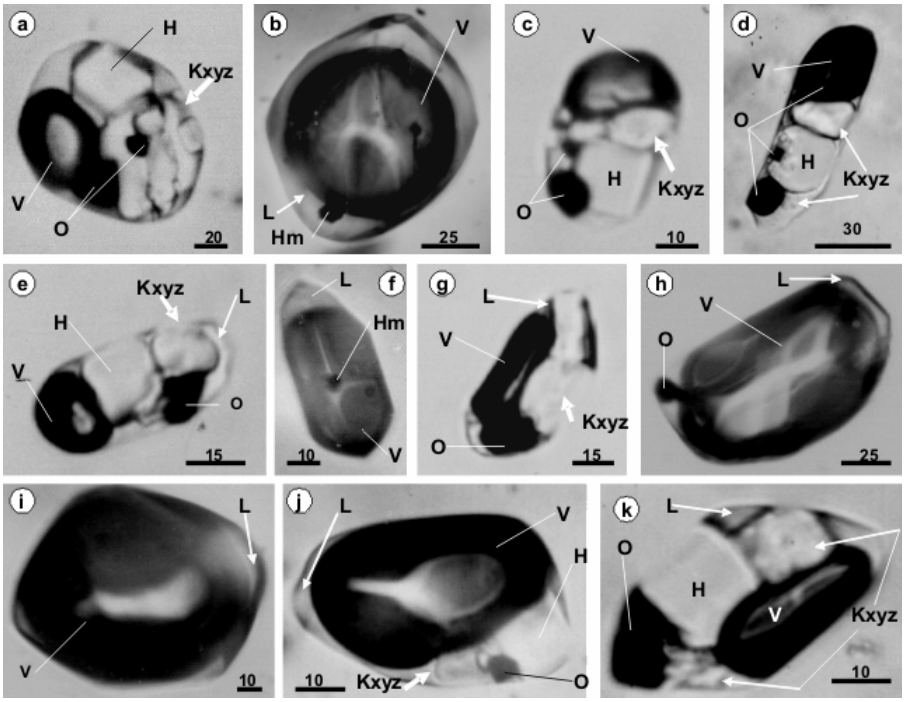

Fig. 7. Hydrous salt melt inclusions and vapor- rich inclusions in quartz veinlets from Rosia Poieni porphyry Cu-Au(Mo) deposit. A thin film of a liquid solution wetting the solid(s) and vapor phases. Notations: H-halite, Kxyz- multiple salt daughter phases including salt hydrates, sylvite , complex solid salt phase(s), sulphate and silicate phase(s), O-opaques, L- liquid, V-vapor, Hm- hematite (specularite). Scale bar in microns.

role of the hydrosilicate gel, silicothermal fluid or "heavy fluid" in the pegmatite and porphyry copper genesis is now under debate and it seems to be one of the main fluid/melt phase involved in mineral precipitation and alteration processes (Wilkinson et al., 1996; Williamson et al., 2002; Vasyukova, 2011; Thomas and Davidson, 2012).

4.2. Hydrous salt melt inclusion

The multiphasic inclusions are representative of the saline rich phases (named hydrosaline melt inclusions by Roedder, 1992), which have been exsolved from the silicate magma by immiscibility as a result of decreasing pressure conditions as well as of a complex chemical composition of the magma (Roedder, 1970; Cline and Bodnar, 1994; Harris et al., 2004). At room temperature, this kind of inclusions contains many solid daughter crystals, a vapor rich phase and variable amounts (zero to few %) of liquid phase. The solid phases include mainly halite, several anisotropic birefringent crystals, silicate minerals, opaques and unidentified mineral species (Fig. 6). The vapor phase is formed by aqueous vapor with small amounts of CO_2 detected by Raman spectroscopy and GC/MS (Pintea, 1996).

The hydrous salt melt inclusions can be primary in origin when they are distributed in growth zones or in random three-dimensional associations. Sometimes, they occur as specific isolated clusters associated with silicate melt inclusions shown in Fig. 5. Frequently, they are distributed in characteristic trails in healed microcracks, suggesting pseudosecondary and secondary origin. Often, they are associated with vapor rich inclusions (Fig.5; Fig. 7). Based upon the phase assemblage at room temperature conditions, the hydrous salt melt inclusions were classified in three main categories, as summarized in Pintea (2001). Saline melt inclusions contain obviously more than five solid daughter phases visible under the petrographic microscope, although a major problem arises here because many of them cannot be identified in this simple way and more analytical techniques were required, like SEM/EDS and PIXE (Damman et al., 1996). Additionally, SEM/EDS analyses were conducted in quartz grains from Deva and Roșia Poieni porphyry copper deposits, showed in Fig. 8 A; some specific spectra are showed in Fig. 8B.

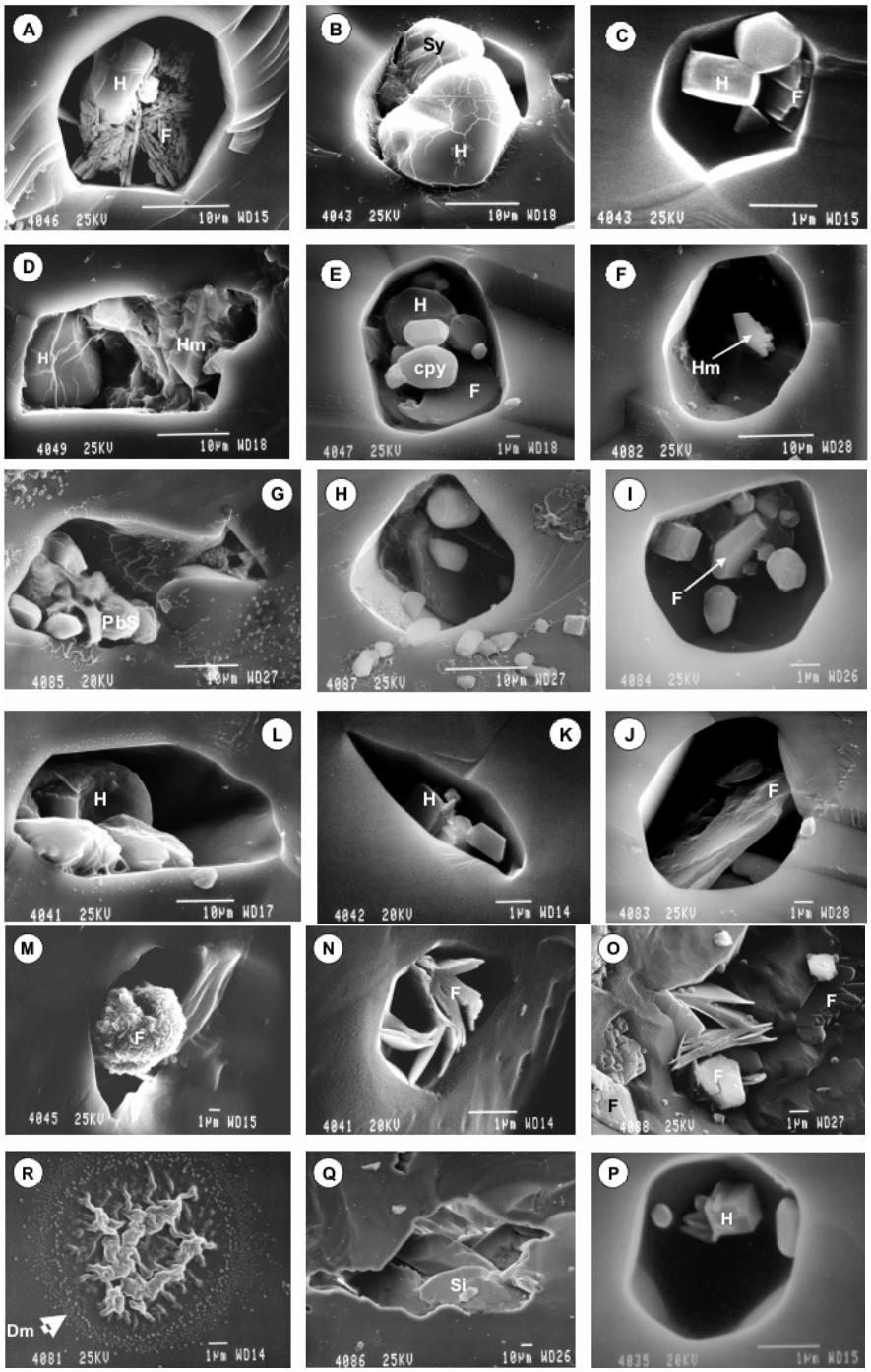

Fig. 8A. Scaninng electron microscope images showing several open microcavity from quartz (A, B, C, D, E, F, G, H, I, J, K, L,M, N, P, Q, R - Rosia Poieni; O-Deva) of the hydrous salt melt inclusions and vapor-rich inclusions filled by solid daughter phases identified by SEM/EDS (SEM JEOL JSM 840 at ETH Hönggerberg- HPT C107-8093 Zurich-1994) as halite (H), sylvite (Sy) feldspar (F), silicate glass remnant (SI), hematite (Hm), sulfides (PbS, Cpy-chalcopyrite and decrepitate mound (Dm) released during the open procedure of the microcavity.

Under the petrographic microscope and during the microthermometric runs, based upon specific melting points (e.g., Table 4) the daughter solid phases can be classified as follows:

a. Transparent, pleocroic grains with blue-green or yellow-greenish birefringence color, which melted first during the microthermometric experiments. They were very sensitive to the laser beam in the Raman analyses, and released instantly a liquid phase (Dubessy pers.comm.);

b. One or more transparent solid grains with orange or yellow birefringence color which melted obviously after halite dissolution;

c. Two or three isotropic crystals, cubic-sharp and octahedral in shape which are the most important solid daughter crystals and are represented by halite, sylvite and K-Fe (Pb, Zn, Mn) Cl salt complex;

d. One or more opaque grains of ore minerals. They can be real daughter crystals and they melted during the microthermometric runs (Table 4 and Fig. 12B), probably being chalcopyrite as was described experimentally by Mavrogenes and Bodnar (1994), or they remain undissolved after the vapor bubble disappearance, suggesting accidental trapping.

4.3. Aqueous vapor-, and liquid-rich inclusions contain a vapor-rich phase being almost monophasic or containing one or more solid transparent or opaque phases represented mainly by halite, hematite, magnetite or chalcopyrite and pyrite (Fig. 7). Obviously, these are associated with various types of melt inclusions as clusters or decorating the healed microcracks as "boiling assemblages". The biphasic (liquid+vapor) type inclusions are related to the fluid phase evolution below 350°-450°C and could be primary in the former silicothermal fluid (now quartz) in a characteristic assemblage, sometimes containing a halite cube or opaque minerals (Pintea, 2010). They are abundant when the epithermal system overprinted the porphyry-type mineralization or are secondary, resulted by thermal decrepitation, necking-down of other inclusion types or during the recicatrization of the secondary microfissures. Epithermal mineralization overprinting the porphyry systems were described as low sulphidation-type at Valea Morii and Bolcana, or high sulphidation-type at Roşia-Poieni and Tălagiu (Pintea, 1996; André-Mayer et al., 2001; Milu et al., 2003; Milu et al., 2004; Kouzmanov et al., 2010; Cioacă, 2011).

4.4. Sulfide melt inclusions

These can be described as globular in shape and formed by pyrite, chalcopyrite, bornite and/or magnetite, occurring as trails, isolated or clustered in the quartz grains, in separate populations or combined assemblages with silicate glass, brine, aqueous and vapor rich inclusions. In fact, they are immiscible (Fe-S-O) melts with significations largely discussed for example by Larocque et al.(2000), Stavast et al.(2006), Nadeau et al., (2010) but can be produced also during the autometasomatic processes or remelting in hydrosilicate rich phases at high temperature and pressure indicated by their counterpart (silicate or saline) homogenization values, mentioned above. Although they cannot be studied by common microthermometry under the microscope, the meniscus-shaped separation at high temperatures could be a good indication that they were trapped in the liquid state (Pintea, 2002; 2010). They were described by their microtextural features as globular variations in quartz in transmitted and reflected light under the microscope, suggesting the presence of Cu-rich pyrite, chalcopyrite, magnetite, pyrrothite, monosulfide solid solution, intermediate solid solution, bornite etc (Fig. 9). They were described in many other porphyry copper deposits worldwide (e.g. Keith et al., 1997; Hattori and Keith, 2001; Landtwing et al., 2005; Halter et al., 2005; Shahabpour, 2006; Audetat and Pettke, 2006; Nadeau et al., 2010; Kamenetsky and Kamenetsky, 2010, the authors suggesting their importance for the ore deposit formation from the magmatic to the hydrothermal stages, no matter whether they are immiscible or fractionated sulfide/oxide phases.

5. Microthermometry

5.1. Silicate melt inclusion microthermometry

It was mentioned above that the silicate melt inclusions contain a clear, transparent and colorless glass and a small rounded vapor bubble. Generally they have small size and obviously are associated with salt melt inclusions and/or vapor inclusions (Fig 10). During the microthermometric experiments the disappearance of the vapor bubble was recorded. Unfortunately, the "pure" silicate melts are difficult to recognize because in almost 90 % of measured runs they contain in variable ratios salt melt and vapor mixtures around homogenization temperature (Fig. 11). Consequently, all silicate melt inclusions contain a few percent of chloride melt even when the homogenization temperature have values ranging between 970° and 1169°C for the measurements given in Table 2A. During cooling, the vapor bubble would nucleate at lower temperature, with 100°-200°C below homogenization value. The chloride globules remain as immiscible droplets in the silicate melt and the vapor bubbles have been renucleated around or inside the chloride phase at the same temperature as mentioned above. The wide range of both kinds of homogenization temperature recorded in the quartz crystals and quartz grains, especially from Deva porphyry copper deposit (Table 2B) shows that some of the higher **Thv** values suggest uncommon trapping conditions or, more probably, were affected by post-entrapment modifications, especially by thermal decrepitation and re-equlibration or heterogeneous trapping (see Disscusion section).

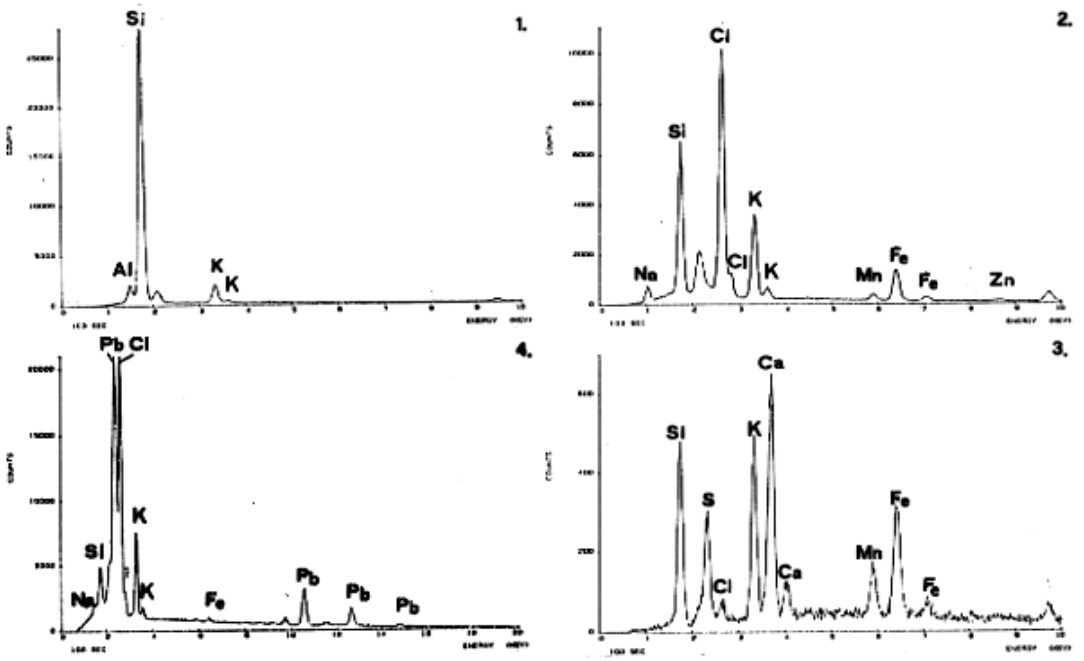

Fig. 8B. Characteristic qualitative spectral diagrams printed for several open cavities analized by SEM/EDS depicted in Fig 8a. 1. K-feldspar, 2.complex chlorides and K- feldspar; 3. K-feldspar, Pb,Fe- chlorides; 4.K,Ca- feldspar, anhydrite, complex chlorides

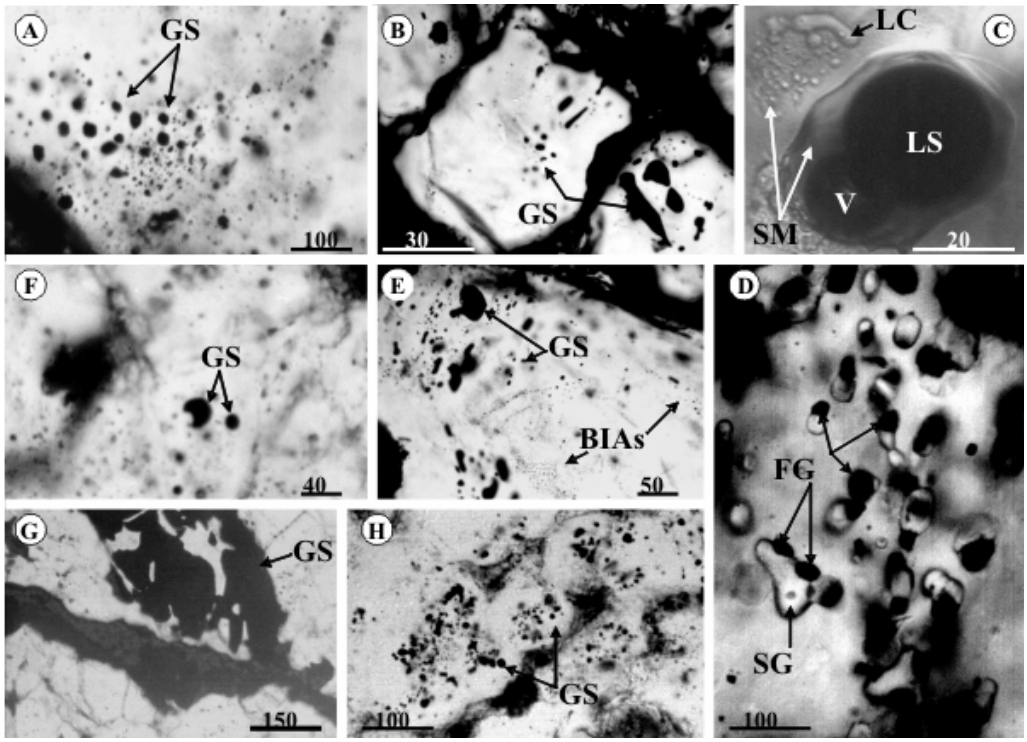

Fig. 9. Opaque (Fe-S-O) immiscible melt globules in transmitted light in quartz from Miocene porphyry copper deposit. A- Rosia - Poeni; B, C (around 1300°C), E - Deva; D, F- Tibles; G,H- Valea Morii. Notations- globular sulphide, SM- silicate melt, LS- liquid sulphide, FG- (Fe-S-O) melt, BIAs- brine inclusion assemblages; V- vapor; black arrow in C indicated a liquid chloride (LC) globula inside the silicate melt. SG- silicate glass or restitic minerals (zircon or apatite -?) in plagioclase from Măgura Neagră – Suplai (Ţibleş massif)- Pintea 2010). Scale bar in microns.

5.2. Hydrous salt melt inclusion microthermometry

In the liquid-free salt melt inclusions, at room temperature, it can be recognized a complex daughter phase assemblage and a vapor bubble which can occupy 40 to 50% volume in the cavities (Fig. 6). It should be noted that the volume estimations of the solid phases are in error because at room temperature the refractive index is close to the quartz host mineral and the contours of the cavities are not easy to follow, but on heating the contour becomes clear after several daughter phases melted on. During the heating experiments, the following phase transitions were recorded:

Tm_1, Tm_2 - The melting points of birefringent blue-green or yellow-greenish grains, which melted first one by one in all microthermometric experiments. The minimum melting temperature values suggests the presence of a hydrate Fe-chloride phase or another similar compound;

Tm_3 -The melting point for an isotropic crystal which was identified as sylvite or other K-rich chloride phase;

Tm NaCl - The dissolution point of halite daughter crystal;

Tm_4 - The dissolution temperature of another group of birefringent solid phases which melted after halite dissolution. They could be anhydrite, K-feldspar or other metal complex chlorides;

Tmo - The melting point of opaque minerals in liquid free hydrous saline melt inclusions. Frequently, they remain undissolved after the disappearance of the vapor bubble. Exceptionally, "in-situ" transformation of an opaque solid phase (magnetite or hematite) during microthermometry, probably a Fe-chloride compound, was noted by Pintea (2009) especially in the samples from Bolcana and Tibles (Pintea, unpubl);

Tmg - At high temperature a silicate rich phase is formed mainly in liquid-free salt melt inclusions. This should be interpreted firstly as a result of dissolution of K-feldspar and other silicate phases formed as daughter crystals. Secondly, another source of silicate liquid phase could be the interaction of the saline fluid with the cavities wall. Nevertheless, this effect seems to be unimportant because the mutual solubility between silicate melt and chloride melt is low, for example anhydrous Na-Ca glasses containing 75% SiO_2 could dissolve a quantity of 0.66 to 2.3 % NaCl at temperature of 750^o to 1400°C (Ryabchikov, 1963; Roedder and Coombs, 1967).

Thp - The temperature of vapor bubble disappearance in salt melt inclusions in which a silicate rich phase is coexistent with a chloride-rich melt. When a salt melt inclusion was heated up to around 1400°C a complex microthermometric behavior has been recorded (e.g. Fig 12A and microphotograph suite in Fig. 12B). The first solid phases dissolved between 60^o to 215°C (Tm_1) or more. This is common for the blue-green birefringent daughter phase, probably represented by salt hydrates.

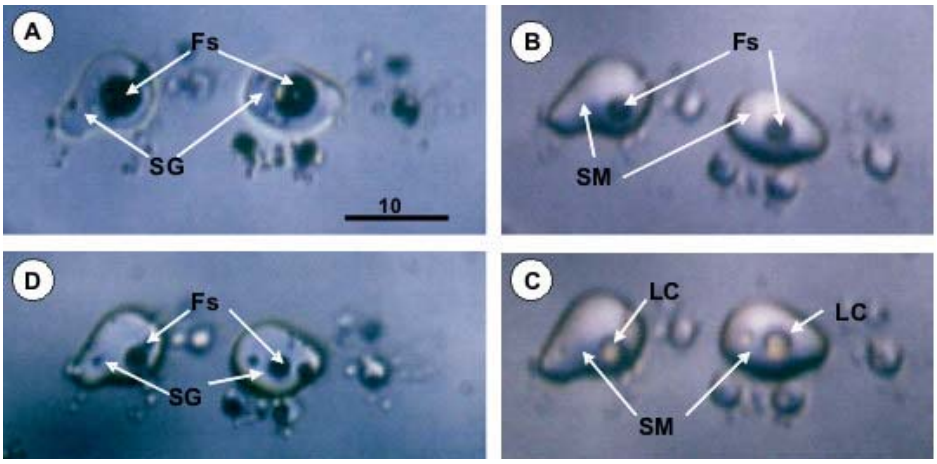

Fig. 10. Microthermometric cycle in complex silicate-hydrous salt melt inclusions in quartz from Deva porphyry Cu-Au(Mo) deposit. At room temperature conditions (A) the microcavities contains a rich silicate glass and a fluid formed by vapor- rich phase, a halite cube and some opaques. On heating the halite melted around 550°C and at 1085°C (B) the fluid bubble is more reduced in volume and contain silicate melt and a dark vapor bubble from which was released around 1267°C a yellow chloride melt (LC) surrounded by a vapor film (dark menisc), (C). Back again to the room temperature (D) the fluid is redistributed in several small dark bubbles and the microcavities have changed ttheir shape. The final homogenization temperature is imposible to be determined accurately because of the permanent immiscibility between the two trapped phases, the silicate melt and the hydrosilicate melt ,+/- vapor rich. Scale bar in microns.

Table 2A. Homogenization temperature measured in simple (glass + vapor) noted as Thv for vapor bubble disappearance in the silicate melt inclusions. Quartz sample from Deva porphyry Cu-Au (Mo) deposit, level-90 (quartz sample collected by S. Boştinescu).

Sample no.	Th_v,°C
D-90-1	1024
"	1050
"	1058
"	1060
"	1070
"	1075
"	1149
"	1150
"	1169
D-90-2	971
"	970
"	994
"	1013
"	1024
D-90-3	1070
"	1075
D-90-4	1149

Table 2B. Homogenization temperature in the silicate glass and hydrous salt melt inclusions trapped in two zones of the quartz crystal indicated with arrow from the selected area in the Fig 11 (ASZ). Thv- vapor bubble disappearance in the silicate glass inclusions (Fig 11.B) and Thp- vapor bubble disappearance in brine liquid-free inclusions from Fig 10.C). Quartz sample from Deva porphyry Cu-Au(Mo) deposit, level-90 (quartz sample collected by S. Boştinescu).

No.crt.	Th_v, °C	Th_p, °C
1	-	1363
2	-	> 1318
3	-	> 1345
4	-	> 1318
5	-	> 1318
6	-	1287
7	> 1365	-
8	> 1267	-
9	1222	-
10	1235	-
11	1232	-
12	1231	-
13	1231	-
14	-	1258
15	1229	-

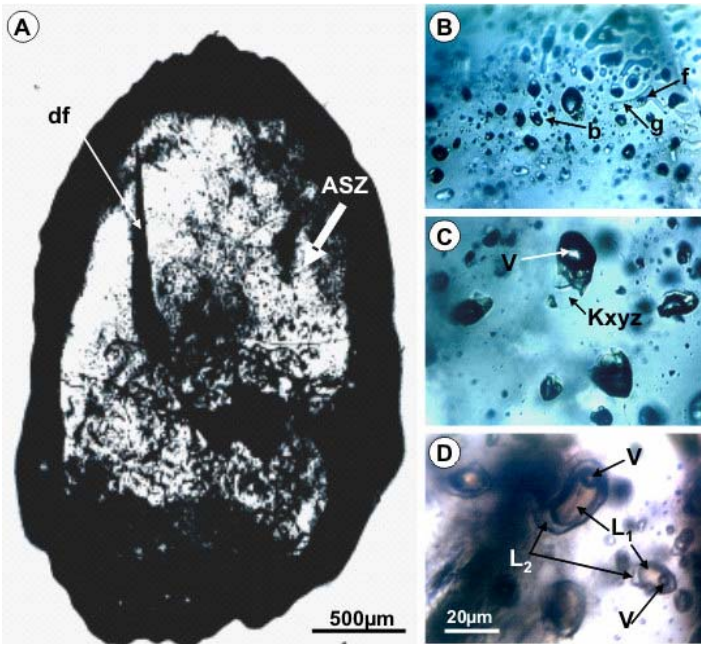

Fig. 11. Individual prismatic quartz crystal (A) double polished in thin section parallel to c axis and shown two distinctive primary assemblages formed by predominantly silicate glass inclusions pictured in (B), and liquid free hydrous salt melt inclusion assemblage in C at room temperature; (D), to high temperature > 1265°C showing three phase equilibrium between silicate melt, salt melt and a vapor bubble. Note that in the selected area indicated by white arrow (ASZ) the silicate glass decorated the border of the growth zone and brine inclusions are situated in the interior of the crystal but both are primary melt inclusions assemblages. df-fissure resulted after the micothermometric heating experiment around 1400°C.

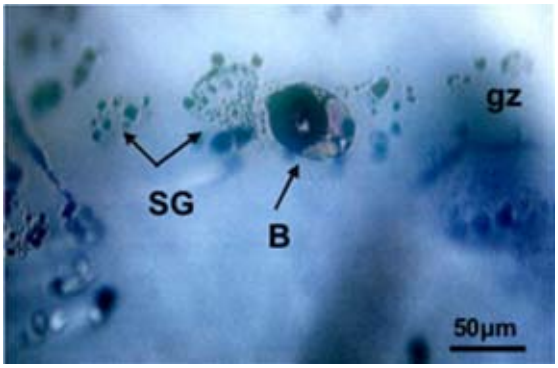

Fig. 12A Hydrous salt melt inclusion (B) trapped in a primary growth zone (gz) decorated with silicate glass inclusions (SG) from Deva porphyry Cu-Au(Mo).See the microthermometry sequences in this brine inclusion in Fig 12B below.

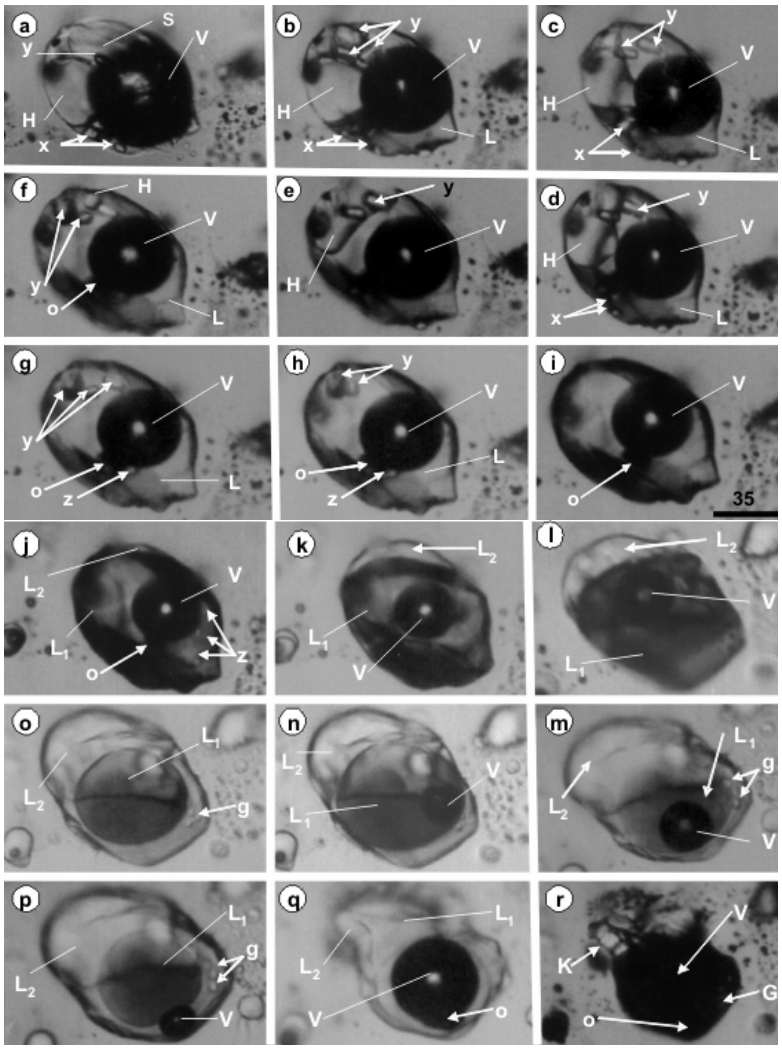

Fig. 12B. Microphotographs of a complete microthermometric cycle in a hydrous salt melt inclusion trapped in a primary quartz growth zone pictured in Fig 12A. a.25°C, b.243°C, c.386°C, d.450°C, e.504°C, f.594°C, g.599°C, h.648°C, i.840°C, j.1086°C, k.1219°C, l.1267°C, m.1284°C, n.1317°C, o.1394°C, p.1284°C, q.1062°C, r.25°C. TmNaCl=598°C, Th(melt-V(melt)=1347°C. Other melting temperature recorded for x (Tm_1=113°C), y (Tm_2=122°C, 288°C-sylvite), z (Tm_4= 602°-840°C), Tmo= 1170°C and renucleated at 1130°C. x,y- chloride hydrates-sylvite solid phase, z- silicate phase(s), and anhydrite-?, O- Fe,Cu sulphide-?, V-Vapor, L_1- chloride liquid, L_2- silicate liquid, g- sulphate globules-?, K- mixture of salt microcrystals renucleated at room temperature. Scale bar in microns. Experiment duration = 5h. Note: Above ca. 1100°C the microcavity have been seriously damaged and their volume increased probably because the chloride liquid phase have dissolved quartz from the walls, and silicate melt liquid increased also in volume, but chloride part seem to be unchanged during the overheating steps. In this case it was estimated that immiscibility occurred at 1086°C, which could be considered as the real "heterogeneous" trapping temperature of the (L+V) chloride mixture and the silicate melt counterpart.

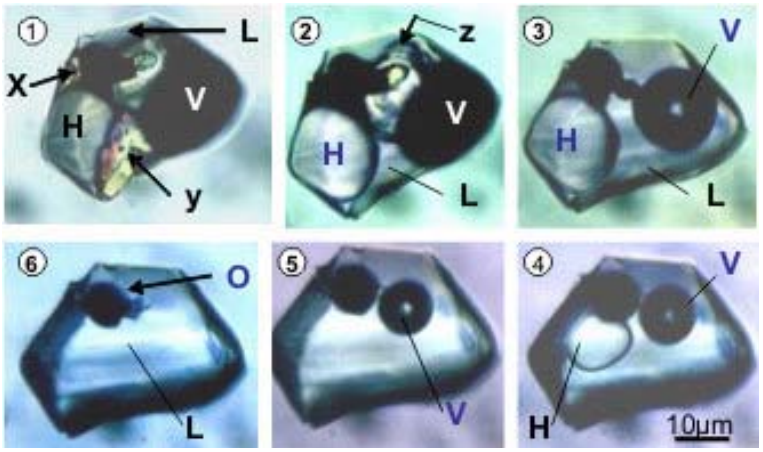

Fig. 13. Hydrous salt melt inclusion with liquid phase at room temperature from Roşia-Poieni porphyry Cu-Au(Mo) deposit, homogenized in "single phase state" in a completed microthermometric run. 1. 25°C), 2. 126°C, 3. 309°C, 4. 575°C, 5. 601°C, 6.750°C, Tm NaCl=585°C, Th (liquid + solid (s) = 749°C; x,y- unknown solid phases, probably salt hydrates and/or complex salts, H- halite, V- vapor, O-opaque (Fe-S-O), L- liquid.

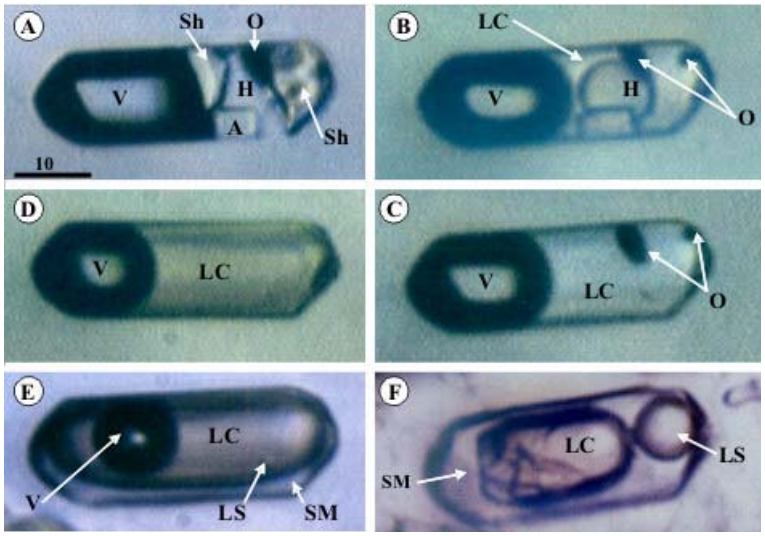

Fig. 14. Microthermometric sequences in hydrous salt melt inclusion from Deva porphyry copper deposit in which three liquid phases were present at homogenization temperature. A.25°C, B.551°C, C. 660°C, D.1149°C, E.1271°C, F.1328°C, TmNaCl=593°C, Tmo=1130°C. At maximum value in F triple immiscibility is shown between silicate melt (SM)-salt melt(LC)-sulphate melt (LS), H- halite, V- vapor, O-opaque, Sh- salt hydrates, A- anhydrite. Scale bar in microns.

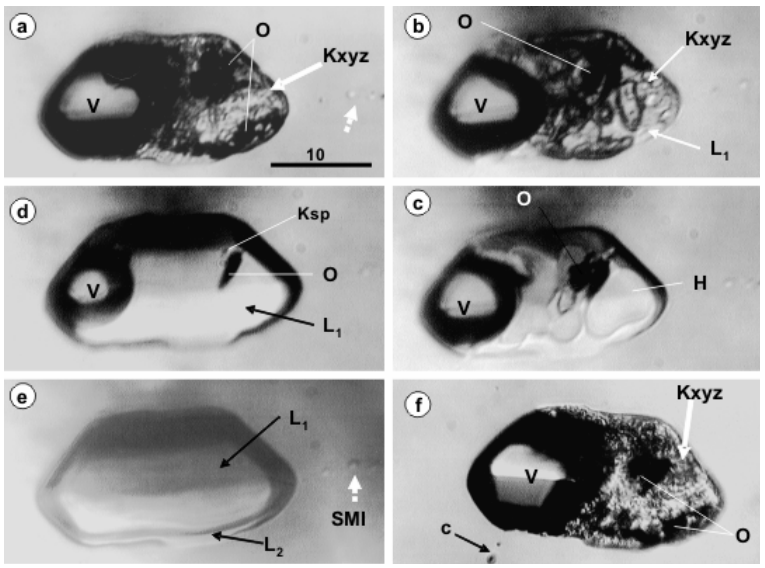

Fig. 15. Sequences of the second microthermometric run, repeated after 2 years in a liquid-free hydrous salt melt inclusion trapped in quartz crystal from Deva porphyry Cu-Au(Mo) deposit.a. 25°C, b.220°C, c.345°C, d.678°C, e.1305°C, f.25°C, Tmh= 555°C, Th=1262°C. Notations: Kxyz- mixture of salt microcrystals with halite (H) dominant solid daughter phase, O-opaques, Ksp- feldspar, L_1- salt melt released by melting of the salt mixture, L_2- a tiny film of silicate melt released by melting the silicate phases, SMI-silicate glass inclusions formed in fissure probably during the first microthermometric cycle (indicated by dashed arrow in a) suggesting a slight leaking process (reequilibration) but the salt melt volume remains almost the same because this recrystallized and filled up the microcavity as in the starting moment (vol in a = vol in f) even if another small fissure (c) is formed in the second cycle (f).

Table 3. Melting temperatures of daughter solid phases and final homogenization temperature in liquid- free brine inclusions from Deva, Roşia Poieni (RP) and Valea Morii (VM) porphyry Cu-Au (Mo) deposits. **- ultrahigh pressure values (see explanation of Table 5). See text for notation explanations.

Deposit/ sample no.	Phase transition temperature (°C)								Salinity (wt% NaCl eq)
	Tm_1	Tm_2	Tm_3	Tm_h	Tm_4	Tm_o	Tm_g	Th_p	
Deva/1	88	189	272	583	658	1116	1209	1234	72
"	181	284	461	578	670	-	-	>1300	73
"	113	122	288	598	602	1170	1086	1347	74**
"	148	260	-	592	654	1136	1088	1326	73**
"	163	253	-	578	708	945	-	1354	71**
"	173	245	277	571	687	-	-	1219	70
"	120	-	-	571	707	1144	1151	1426	70**
"	130	277	324	589	696	1006	1326	1404	73**
"	90	216	316	587	607	1013	1345	1405	72**
"	130	223	374	588	704	1050	1345	1413	73**
"	184	256	362	570	665	1073	976	1170	70
"	130	276	362	581	674	1073	976	1322	71**
Deva/ 2	-	243	-	589	-	-	1224	1332	73**
"	120	175	268	575	643	932	-	1115	71
"	120	175	273	576	698	945	-	1160	71
"	170	271	276	569	698	739	1362	>1354	71**
R P/18	215	240	-	583	-	1010	-	1038	72
VM /1	90	-	256	495	830	976	1115	1151	59
"	133	-	285	531	908	1088	1115	1225	64
"	90	238	343	468	-	-	-	1133	56

The second solid phase which has almost the same optical properties (slightly greenish) dissolved at high temperature between 122°-284°C (Tm_2- probably sylvite when is isotropic). The next solid daughter crystal, assumed to be a complex (K, Fe, Mn - Cl) melted obviously between 256° to 461°C (Tm_3). On further heating, halite melted between 412° to 607°C (Tm NaCl) for the selected microthermometric runs in Tables 4 and 5. The latest transparent phases with yellow or orange color under cross polars were melted at temperature higher than 600°C, and sometimes around 900°C.

They might be represented by Fe-chloride, anhydrite or a silica-rich phase (K-feldspar, mica, quartz etc.).The liquid-rich phases appear in a wide temperature range between 976° to 1362°C and could be interpreted as the result of the silicate daughter phases dissolution and/or interaction between salt melt and inclusion walls. The melting of the opaque minerals took place in a wide range of temperature, between 890° and 1170°C as shown in the suite of selected values from Table 3 and Table 4. A more relevant phase transition, which was recorded usually in saline melt inclusions during heating operations, is the formation of a silicate liquid rim around the salt melt droplet. A tiny film of silicate liquid phase start to appear at temperature near 1000°C or more, and the volume increased relative to the inclusion volume as a function of the partial homogenization temperature, i.e. temperature of the vapor bubble homogenization in the salt globule, Thp. If this temperature is around 1400°C or even more, the silicate liquid phase can occupy more than 50% of the cavity volume. Perhaps some silicate-rich liquid is released by wall dissolution, but this is low and cannot exceed the mutual solubility limit. The volume increase of the cavity was only in the order of 5 - 10%, slightly more at the highest temperature in the stage. On further heating, the vapor bubble disappeared in a wide range of temperatures and, after that, in salt melt inclusions free of liquid at room temperature, the silicate-rich phase and a salt +/- sulfate globule coexisted (Fig 14). An opaque sulfide globule was often separated inside the silicate melt during the microthermometric run around 1300°C in many inclusions, especially in the quartz from Deva PCD (Pintea, 2002, e.g. Fig. 9 C). On cooling,

the vapor bubble nucleates first and, after that, one by one, the solid phases beginning with the solidification of the silicate glass around chloride melt + vapor phase. At the room temperature conditions all the initial phases should be present but the shape of the cavities and the arrangement of the phases is very different from the initial state before heating experiment (Fig 12B).

For the saline melt inclusions with liquid phase at room temperature, the microthermometric behavior is slightly different from that presented above (see Fig. 13 as an example). They contain also a complex solid daughter phase assemblage, a vapor bubble and a small amount of liquid phase, but sometimes the birefringent phase is missing and the opaque grains remain (more undissolved after the vapor bubble disappears (Table 4).

The silicate liquid phase meniscus is seldom formed after homogenization temperature and commonly the vapor bubble disappeared before halite dissolution (i.e. halite homogenization).

Table 4. Microthermometric data for hydrous salt melt inclusions with small amount of liquid phase at room temperature in quartz sample from Roşia Poieni (RP), Bolcana (B),Valea Morii (VM), Talagiu (T), Ţibleş Massif-Măgura Neagră-Suplai (Tb) phorphyry copper deposits. See text for explanations.

Location /sample no.	Phase transition temperatures (^{o}C)					Salinity (wt% NaCl eq.)
	Tm1	Tm3	Tmh	Thv	Tmo	
B/11	166	284	516	1094	890	62
“	-	-	550	1161	1081	67
“	175	274	574	1174	996	70
“	166	274	526	1074	929	64
“	175	275	574	1216	1158	70
“	173	235	534	1158	1098	65
B/17	130	275	549	817	-	67
“	132	270	571	842	-	70
RP/18	60	256	585	749	-	72
“	154	240	558	724	-	68
“	148	240	561	729	-	69
“	130	257	562	730	-	69
“	150	238	579	760	-	71
“	-	256	583	772	-	72
“	215	240	506	506	-	61
“	225	290	578	765	-	71
“	138	209	532	773	-	64
RP/25	170	296	455	1083	-	54
“	182	297	460	1136	-	54
“	130	-	412	665	-	49
“	137	-	422	676	-	50
“	95	-	541	753	-	66
“	150	-	549	775	-	67
VM/1	90	256	495	632	-	59
“	133	285	531	748	-	64
“	-	337	607	656	-	75
“	90	296	555	668	-	68
“	115	296	587	680	-	72
T/23	-	259	523	618	-	63
“	-	-	553	1037	-	67
Tb47	-	-	573	705		70
“	-	-	594	872	-	73
“	-	-	594	1070	-	73
“	-	-	565	830	-	69
“	-	-	519	682	-	63

Table 5. SoWat calculation showing the main characteristics of the trapped phases in the hydrous salt melt inclusions. The physical phase state (single phase state, L-liquid, V-vapor, H-halite) were observed at homogenization temperature values. For "single phase state" trapping was homogeneous, for L+V or V+H trapping was heterogeneous or the cavities have been decrepitated during the microthermometric runs or natural reheating.

No crt	Th_p,°C	P, kbar	Liquid		Vapor		Single phase		Initial fluid state
			W_L	D_L	Wv	D_V	Ws	Ds	
1	1262	12.8	-	-	-	-	68	1.2	single phase
2	1234	8.2	-	-	-	-	72	1.2	single phase
3	1219	6.3	-	-	-	-	70	1.2	single phase
4	1170	2.7	-	-	-	-	70	1.1	single phase
5	1115	2.0	71	1.1	10	0.4	-	-	V+L
6	1160	2.2	-	-	-	-	71	1.1	single phase
7	1038	1.6	-	-	-	-	72	1.1	single phase
8	1151	2.5	59	0.9	17	0.5	-	-	V+L
9	1225	7.0	-	-	-	-	64	1.1	single phase
10	1133	2.5	56	0.9	18	0.5	-	-	V+L
11	1094	2.2	-	-	-	-	62	1.0	single phase
12	1161	2.4	67	1.0	15	0.4	-	-	V+L
13	1158	2.4	-	-	-	-	65	1.0	single phase
14	817	1.0	-	-	-	-	67	1.0	single phase
15	842	1.0	-	-	-	-	70	1.0	single phase
16	749	0.7	-	-	-	-	72	1.1	single phase
17	724	0.7	68	1.1	0.8	0.2	-	-	V+L
18	729	0.7	69	1.1	0.8	0.2	-	-	V+L
19	730	0.7	-	-	-	-	69	1.0	single phase
20	760	0.8	71	1.1	0.8	0.2	-	-	V+L
21	772	0.8	-	-	-	-	72	1.1	single phase
22	506	0.3	61	-	0.1	0.1	-	-	V+H
23	765	0.8	71	1.1	0.9	0.2	-	-	V+L
24	773	1.0	-	-	-	-	64	1.0	single phase
25	1083	2.3	54	0.9	17	0.6	-	-	V+L
26	1136	2.5	54	0.9	18	0.6	-	-	V+L
27	665	0.9	-	-	-	-	49	0.9	single phase
28	676	0.9	50	0.9	2.3	0.3	-	-	V+L
29	753	0.9	66	1.0	1.3	0.2	-	-	V+L
30	775	0.9	66	1.0	1.3	0.2	-	-	V+L
31	632	0.7	-	-	-	-	59	1.0	single phase
32	748	0.9	-	-	-	-	64	1.0	single phase
33	656	0.5	75	1.3	0.2	0.1	-	-	V+L
34	668	0.6	68	1.1	0.4	0.2	-	-	V+L
35	680	0.6	-	-	-	-	72	1.2	single phase
36	618	0.6	-	-	-	-	63	1.1	single phase
37	1037	1.8	-	-	-	-	67	1.0	single phase
38	705	0.65	70	1.2	0.5	0.2	-	-	V+L
39	872	1.7	48	0.9	16	0.5	-	-	V+L
40	1070	1.6	73	1.1	6	0.3	-	-	V+L
41	830	1.0	69	1.1	2	0.2	-	-	V+L
42	682	0.8	-	-	-	-	63	1.1	single phase

Note : Ws-composition of single phase state in wt% NaCl eq.; Ds-single phase density in g/ccm; WL-composition of the liquid phase in wt% NaCl eq.; DL- liquid phase density in g/ccm; Wv- vapor phase composition in wt % NaCl eq.; Dv- vapor phase density in g/ccm. Note: For the inclusions labeled ** in Table 3 the density calculated values were 0 g/ccm, that is an uncertain significance, and these data will be probably avoided from further geological interpretation.

Table 6. Bulk crush-leach analyses of released fluid from quartz veins at Rosia Poieni porphyry Cu-Au(Mo) deposit (Pintea unpublished IGR-report arch .-1998). Sample No. 11* and 18* have been measured for δ37Cl ratio, which ranged between -0.28‰ and -0.43 ‰, respectively (Pintea et al., 1999b)

Sample no.	Altitude (m)	KCl wt%	$CaCl_2$ wt%	$FeCl_2$ wt%	NaCl wt%	$MgCl_2$ wt%
41	1060	24.17	24.33	24.81	13.88	12.81
8	1030	13.46	64.20	12.37	6.22	3.75
11*	1030	23.72	40.20	15.53	12.97	7.58
45	1030	13.06	25.30	52.63	5.08	3.93
16	1000	13.41	60.39	15.29	4.86	6.05
18*	1000	36.10	32.57	13.08	18.22	0.03
20	1000	39.51	25.66	10.99	17.51	6.33
43	985	26.61	40.75	19.30	6.24	7.10
29	970	17.00	35.93	32.85	6.54	7.68
31	970	19.64	43.06	24.55	7.68	5.07
33	970	28.67	39.86	12.84	8.96	9.67
27	970	26.90	44.65	16.01	8.35	4.09

This kind of homogenization is characteristic for the "halite trend solution" and an explanation for this trend is the precipitation of KCl-bearing halite prior to entrapment, mainly because of boiling processes (Cloke and Kesler, 1979; Quan et al., 1987). The selected values from Table 3 and Table 4 above come from a huge number (more than 500) of measurements (i.e. microthermometric cycles) and some of them (n=350) were projected recently in a Salinity-Homogenization temperature diagram (Pintea, 2012).

6. Discussion and conclusions

6.1. Melting and homogenization temperatures

The complex microthermometric behavior during the heating runs was recorded in liquid-free salt melt inclusions. There, the melting temperatures of almost all solid daughter phases were measured, including the formation of silicate liquid meniscus surrounding the salt melt, and also the opaques melting temperatures (e.g. Fig. 12B-j). These phases have the highest (excessive) final homogenization temperature in the salt liquid phase and show strong evidence of heterogeneous trapping (immiscibility). As the liquid content in the brine inclusions is more visible (Table 4) the number of melting points decreased and the opaque phase obviously could not be melted before the vapor bubble disappearance. Also, the liquid silicate meniscus is not visible at the homogenization temperature. The main questions that arised is if the melting temperature of the opaque phases recorded are the real precipitation temperatures of those phases in the inclusions or have they already been entrapped in the solid state (as "micro-nuggets" or "step daughter minerals"). Opaque sulfide globules floating in the silicate melt inclusions coeval with salt melt inclusions were also observed, especially at highest homogenization temperatures (Pintea 2002, e.g. Fig. 9C). It is a common feature that during the alteration of the mafic phenocrysts as biotite, hornblende, pyroxene or during total feldspar destruction stage, a Fe-rich sulfide phase can be released and the globular appearance suggested the initial liquid phase state (Shahabpour, 2000). These minerals would be involved in the redistribution of ore elements together with silicate, saline and aqueous rich phases during the magmatic-to-hydrothermal processes and their study showed that they have great importance in developing economic ores (e.g. Keith et al., 1997; Hattori and Keith, 2001; Landtwing et al., 2005; Halter et al., 2005; Audetat and Pettke, 2006; Nadeau et al., 2010; Kamenetsky and Kamenetsky, 2010.

Another problem is related to the silicate liquid rim released around the salt melt from the silicate daughter minerals melted (dissolved) during heating. This can be the effect of the immiscibility of the two phases (trapped together in various proportions) or maybe the silicate liquid was generated by the reaction between the inclusion wall and the released salt rich fluid formed by the melting of the saline daughter phases inside the inclusion.

The first melting point is representative for several birefringent grains probably salt hydrates and then a slight birefringent phase occupies almost the same volume as the halite daughter

phase, probably a multiple salt phase. Sylvite is very difficult to be seen because of its small volume and high transparency. Anhydrite or even the silicate daughter phase cannot be identified by normal optical microscopy. Finally, only the temperature of the halite daughter phase dissolution can be precisely recorded, therefore, the system H_2O-NaCl is obviously used to modeling the fluid phase equilibrium in brine inclusions. Nevertheless, as it is known, the composition of these is expressed as wt% NaCl equivalent and every evolution path (or snapshot) isochor-isopleth in a P-T plane is related to this system. This is a good approximation (e.g. Bodnar et al., 1985) but we do not have any data, yet, about the importance of the solubility of salt hydrates, (K, Fe, Mn)-Cl phase, KCl, anhydrite, quartz, micas, sulphide, oxide phases in the mother salty/silicate liquors of the hydrous salt melt inclusion. Moreover, the final homogenization temperature is higher than any liquidus temperature, considering the composition of the host magma, especially for the liquid-free saline inclusions in Table 3. Even if the salt-rich inclusions show re-equilibration after the high temperature homogenization runs (Fig. 12B, Fig. 14), the salt liquid + vapor is surrounded by the viscous silicate liquid and remain separated as immiscible phase, thus the temperature at the vapor bubble disappearance could be the trapping temperature, if the initial fluid was a homogeneous salt melt (Table 5).To justify immiscibility between silicate and salt melt, in this research, the microthermometric runs were obviously completed until the separate phases were coexistent and the liquid homogenization temperature (Thp) was used to calculate salinity using the new available software (e.g. Driesner and Heinrich, 2007). The microthermometric data from Table 3 suggest, firstly, that salt melt inclusions without visible liquid phase at room temperature conditions contain the most complete solid daughter phase assemblage. All of these phases dissolved during heating runs in the presence of a vapor phase and suggest homogeneous trapping, and they renucleated in reversed order when temperature in the stage decreassed to the room conditions. Moreover, the petrographic observations showed a common distribution for the inclusions of primary origin (Roedder, 1984), and that salt melts are coexistent or trapped together with silicate melt. The salt melts floated as globules in the more dense silicate melt, taken into account the low mutual solubility between these two melts. That is, during magma crystallization, salt melt will exsolve the first, and then, because of increasing water content, the chemistry of the salt melt would be drastically changed. This fact is illustrated in Table 4, showing the melting temperatures recorded in salt melt inclusions, where a variable amount of water is present as a liquid film visible at room temperature. In these inclusions, many of the solid daughter phases are missing and/or the opaque phases remains undissolved after the vapor bubble disappearance, and also the silicate liquid phase is not released during heating runs. Probably, when only salt is exsolved from magma, much more metal comes out as chloride complexes and probably precipitates as oxides and sulphides depending on the initial S content of the melts and on the oxygen fugacity controlled by hematite-magnetite (HM) buffer (Eugster, 1986, Burnham and Ohmoto, 1980). The presence of magnetite and hexagonal red flakes of hematite (specularite) is a common fact in salt melt inclusions from PCDs (Roedder, 1981; Fig. 7, Fig. 5 this study). During the microthermometric runs in the salt liquid-free inclusions, these generally melted and renucleated constantly on decreasing temperature. But they remained undissolved in the hydrous salt melt inclusions, where a film of liquid solution is visible. The ultrahigh Thp values recorded in our sample from the porphyry Cu-Au(Mo) deposits from Metaliferi Mountains could be related also to many factors such as post-entrapment modification of the microcavities by necking-down, stretching, thermal decrepitation and leakage-in or out during reequilibration (Hall and Sterner, 1993; Audetat and Günther, 1999; Bodnar, 2003). On the other hand, the stability of vapor bubbles of the hydrous salt melt inclusions could be influenced probably by their chemistry. For example, Webster and Mandeville (2007) emphasized recently that the high temperature homogenization in brine inclusions, i.e. the persistence of the vapor bubble to high temperatures, could be done by the presence of the $CaCl_2$ and $MgCl_2$ when the fluid were exsolved from mafic melts, which in their turn were subjected to large ranges of P-T conditions. This interpretation is concordant with the bulk crush-leach analyses of the solutions extracted from quartz, sampled at Roşia Poieni (Table 6, Pintea-unpublished) and Ţibles (Pintea et al., 1999a) porphyry copper

systems, where the predominant chlorides are $CaCl_2$, $FeCl_2$, and not NaCl, as was obtained by microthermometry of the individual hydrous salt melt inclusions. More recent analyses by LA-ICP-MS in complex brine inclusions and vapor-rich ones as well, from the Western Carpathians (Kodera et al., 2012; 2014) showed unusual proportions of Fe-K-Na-Cl (i.e. FeCl>KCl>NaCl).

6.2. Fluid-melt immiscibility in porphyry copper genesis

The milestone orthomagmatic model elaborated by Burnham (1979) postulated that a granodioritic magma containing 3.0 wt% H_2O has been emplaced in a subvolcanic environment and undergone cooling to below solidus temperature, under the saturated carapace, labeled "S_1" in his famous Fig 3.5a. These picture sequences are then reloaded and discussed everywhere the orthomagmatic model is invoked (see recent data of Becker et al., 2008, Bodnar, 2010).The inner temperature in that model is fixed at 1025°C and the line 1000°C is the limit of the melt with the solidifying carapace where biotite and hornblende start to crystallize in the outer zones, releasing silica, which leads to the crystallization of quartz (Burnham, 1979). Some of this quartz will be accumulated in the vein networks, which are formed outward by a sequence of explosion and brecciation of the retreated-downward saturated carapace. This is why we assumed that the small quartz grains protruded in the dilating endocinetic fissures (veinlets) contain multiple overgrowth zones (Pintea, 2009). Moreover, in the Burnham's model (1979) was evidenced that the second boiling process (resurgent boiling) is characterized by the reaction H_2O-saturated melt → crystal + vapor, which involved a pressure increase under the carapace as cooling and crystallization proceeded. The inner pressure can reach any value (i.e → ∞) and would be very high mainly in isolated small pockets of H_2O-saturated magma. Despite the fact that our homogenization temperature is far away from the liquidus temperature used by Burnham in his model, the pressure calculated from these are in accord with the assertion made above. So we can explain these ultrahigh P-T data in several ways and one of these is the stress conditions under the saturated carapace inside the liquid magma batch which can be recharged by ultrahot silicate liquids from underlying mafic magma coming from different depths generated first in the MASH zone (Cloos, 2001; Campos et al., 2002; Richards, 2003). A strong argument in favor of this recharging process with high P-T fluids is based on the fact that for hydrous salt melt inclusions, the saline rich melt is always surrounded by the viscous silicate melt as immiscible phase, so that, during the high temperature microthermometry, the saline rich phase cannot change its initial volume and the measured Thp seems to be correct (Fig. 14). Even in the picture sequences from Fig. 15, where a small crack is filled with silicate melt inclusions (SMI) it is evident that the chloride phase has not leaked around because the silicate liquid acted as a protector wall and the saline phase remained in constant volume and recrystallized and refilled the cavity as it was initially, before starting the microthermometric experiment. Another plausible explanation for the accuracy of our data in terms of P-T trapping conditions is the fact that the highest values are characteristic for the sample coming from Deva porphyry copper system, which occurred near the South Transylvanian fault system that, as the Western fissure in the Andes (Campos et al., 2002) is a deep fault system developed during subduction in the back arc region. Even the geological profile at Deva porphyry is suggestive for this tectonics as it looks like a narrow dyke (Ivăşcanu, et al., 2003) probably ascended through a deep fault system. Therefore, it is possible that the quartz grains in the veinlets from the Deva stockwork (high pressure breccia body at -90 m level underground) mentioned by Boştinescu (1983, unpublished report) originate from different depths, as suggested by the high P-T conditions (Table 2, Table 3). By using the SoWat software (Driesner and Heinrich, 2007), it was possible to find out that the majority of the hydrous salt melt inclusions contain, at the homogenization temperature, a single homogeneous liquid phase (Table 5). Other hydrous salt melt inclusions show liquid (L) and vapor (V) coexistence, which could be an indication of boiling at the trapping moment, when vapor and liquid were enclosed heterogeneously in the same cavity. Rarely, vapor and solid halite crystals were trapped together; this is the case presented recently by Muntean and Einaudi (2000) for the porphyry-Au deposits in the Maricunga belt (Chile) and by Kodera et al. (2012), in the Western Carpathians, for the same type of the deposit. In both mentioned examples, only high salinity brine inclusions were coexistent with vapor-rich

inclusions in trails, and there is no mention of immiscibility between fluid and the silicate melt, as in our case study. In our interpretation, the hydrous salt melt inclusions are the result of heterogeneous trapping at different depth, below the actual porphyry systems as the calculated pressure suggested (Table 5). Additionally, it was emphasized (Pintea, 2009), based upon microtextural evidences, that adjacent quartz grains contain different kinds of fluid and melt inclusion assemblages suggesting that they were crystallized at different depths and brought together in the same fractures by successive fluid flushing events. Alternatively, the quartz grains in the veinlets recrystallized from the hydrosilicate gel (silicothermal fluids) or "heavy fluid" as was emphasized by Vasyukova et al. (2008) and Vasyukova (2011).

The ultrahigh P-T ($\geq 900^{o}$ -1100°C and 0.3-12.8 kbars) data reported in this research could be related to the metasomatised lithospheric mantle above the astenospheric wedge (802^{o}-1416°C, 3.2-9.7 kbars) in a W-directed subduction environment in the Eastern Carpathians (Kovacs, 2002; Seghedi et al., 2004; Doglioni et al., 2009) and to the extension and partial melting of the mantle source and metasomatism in the Apuseni Mountains (Richards, 2009; Harris et al., 2012). These data and settings suggest the separation of hydrous salt, silicate, sulfide and aqueous fluids by immiscibility from the partialy molten mafic rocks at the base of the Earth crust. In this respect, at magmatic to hydrothermal transition concomitantly with the second boiling process and fluid phase separation, a wide range of autometasomatic and remelting features were also described in these two regions (Pintea, 2010). Moreover, data about high pressure at magmatic temperature come out from high density water-rich inclusions study from central Slovakia, in Western Carpathians (Naumov et al., 1996). The authors mentioned a water pressure of 5.6 to 15-17 kbars at 800^{o}-900°C, during magma crystallization. However, these high pressure values were questioned by Davidson and Kamenetsky (2007), and they argued that "the presence of single-phase aqueous bubbles in melt inclusions is a metastability effect". The metastable superheated solutions were studied by isochoric experimental runs in synthetic fluid inclusions synthetized at 7.5 kbars and 530^{o}-700°C, and demonstrated that "natural solutions can reach high levels of superheating" (Shmulovich et al., 2009). Also, the presence of silicate globules as (re)melting products in the porphyry copper deposits from Metaliferi Mountains and Eastern Carpathians (e.g. Ţibleş massif), as well as their formation in many experimental studies (e.g. Antignano and Manning, 2008) are strong arguments that our microthermometric records could be the real trapping P-T conditions for silicate melt and hydrous saline inclusions assemblages (Table 2, 3, 4 and 5). Anyhow, the excessive values labeled * * in Table 3, probably would be avoided from further interpretation, these being related mostly of post-entrapment processes. Therefore, there still remain a lot of debatable issues regarding the fluid/melt separation and evolution during the porphyry copper genesis in the studied regions of the Carpathians.

In summary, the silicate and hydrous salt melt inclusions study from the porphyry Cu(-Au,-Mo) deposits of the Metaliferi Mountains and Ţibleş massif in the Eastern Carpathians (Romania) presented in this review could be summarized as follows:

- The evidence of liquid magmatic immiscibility between silicate melt and salt melt is based on the contemporary occurrence of inclusions within the quartz crystals. The phases in the inclusions include silicate melt, hydrous salt melt, (Fe-S-O) globules and water-rich fluids trapped in various proportions in separate and/or coeval inclusions.
- The temperature of vapor bubble disappearance in silicate glass inclusions and the temperature of the silicate liquid rim formation surrounding the salt melt globule, seem to be the real trapping temperatures of the melt inclusions, mostly in the interval 1000°-1100°C. Neverthelles, they seems to have a reasonable geological meaning only if we assume that they were trapped from different magma batches, where ultrahigh P-T mafic influx invaded the MASH zone, from which the andesitic melt was segregated, then ascended and crystallized by retreating downward, as it was postulated by Burnham's model. An exception is the case of Deva porphyry copper deposit, which is emplaced close to the South-Transylvanian deep fault system, as is the Western fissure in the Andes, where porphyry copper system were also developed and show similar characteristics of the fluid and melt inclusions (Campos et al., 2002). The multiple stages of the porphyry copper evolution, starting deep in the Earth's

crust were emphasized by many authors, worldwide, e.g., Richards (2003, 2009) and Cloos (2001).
- Usually, quartz crystals are zoned because of the retreating downward crystallization process and the mixture of silicate melt, salt melt + vapor were exsolved sequentially during magma emplacement in the inner part of the shallow intrusives where the ore is located. This is composed of myriads of small veins in a brittle structure, filled up with quartz - pyrite, quartz - magnetite - chalcopyrite, quartz - bornite – chalcopyrite, and is associated with the potassic alteration in the host rock, consisting of K-feldspar, biotite, magnetite; the potassic alteration may be obliterated by subsequent alteration mineral charcteristic for the phyllic, propylitic or argillic alteration facies.
- The saline melts can be sometimes considered as metal solvent solution because in most microthermometric runs, depending on the water content, the opaque daughter minerals were dissolved during heating and reprecipitated on cooling; otherwise they remained undissolved or became globular opaque melt phases at very high temperature, i.e. around 1300°C.
- Alternatively or complementary, the silicate melt, and hydrous salt melt inclusions plus vapor- and liquid-rich inclusions seem to be the products released by the reaction between a supercritical fluid(?), which separates in low and high salinity fluid phases, and the crystallizing magmatic minerals during the autometasomatic and remelting processes. The high P-T ($\geq 900^{o}$-1000°C, 0.3-12.8 kbars) conditions of such processes would be correlated with the existence of a "mafic nucleus" mixed or mingled with the felsic melt in intermediate magma chambers and recycled by autometasomatism, as subtle mechanism of porphyry-copper deposits generation inside the shallow subvolcanic structures. In these processes, the fluid phases were transported by hydrous silicate melts (silicothermal fluids-Wilkinson et al., 1996, "heavy fluid"-Vasyukova, 2011) and trapped in crystallized quartz in magmatic to hydrothermal conditions; globular sulfide were released in the mean time and beneficiated the ore deposit metal content.
- In many PCDs from Metaliferi Mountains and Ţibles massif in Eastern Carpathians, a meteoric water-dominated convective system was recognized being centered on the "protore" zone and surroundings, composed by veins, breccias, stockworks, where the primary ore deposit (spatially corresponding with the potassic alteration zone) was altered, transported and reprecipitated as epithermal products of high sulfidation and/or low sulfidation type.
- The ultrahigh P-T ($\geq 900^{o}$-1000°C, 0.3-12.8 kbars) magmatic immiscibility, discussed in this paper, was generated in specific geodynamic conditions during the middle Miocene extensional regime in the Apuseni Mountains, which caused decompression melting in a geotectonic setting modified by clock-wise rotation of the intra-Carpathian blocks coupled to the astenosphere upwelling and a higher thermal regime (Roşu et al., 2004; Seghedi et al., 2010; Harris et al., 2013). The genesis of the Măgura Neagra-Suplai porphyry copper system from Ţibles Mountains in Eastern Carpathians is still under debate (Udubaşa et al., 1984; Pintea et al., 1999a).

Acknowledgements. This work was supported initially by Swiss National Found for Eastern Countries by SNF grant 2 – 77 – 791 – 93 at Institute of Mineralogy and Petrography from Swiss Federal Institute of Technology Zurich. Analytical and microthermometric data measured at ETH - Zurich is part of a Ph D. thesis undertaken between 1990-1996 at the University of Bucharest under the supervision of E. Constantinescu. The author is grateful to Professors E. Constantinescu (University of Bucharest) T.M. Seward (ETH Zurich) and J.L.R. Touret (Vrije Universiteit, Amsterdam) for help and guidance during Ph D. project work time. I thank Dr. J. Dubessy for the Raman analyses at CREGU.GS CNRS, Nancy France. The earlier version of manuscript was improved after valuable observations made by E. Campos, R. Clocchiatti, C.A. Heinrich and J.L.R. Touret for which I express my gratitude. Others improvements come from two anonymous revivers (A and B) from a special Chemical Geology issue, on Melt Inclusion, 2001 coordinated by dr. E. Hauri from Carnegie Institution, Washington for which I am indebted too. I express my gratitude to the two RJES annonymous reviewers and editorial handling by M. Munteanu, which substantially improved the final version of this review.

References

Anderson A.T.Jr., 1991. Hourglass inclusions: Theory and application to the Bishop rhyolite tuff. American Mineralogist, 76, 530 - 547.

André-Mayer A.S., Leroy J.L., Marcoux E., Lerouge C., 2001. Inclusions fluides et isotopes du soufre du gisement Cu-Au de Valea Morii (Monts Apuseni, Roumanie): un télescopage porphyre-épithermal neutre? C. R. Acad. Sci. Paris, Sciences de la Terre et des planètes, 333, 121-128.

Antignano A., Manning C.E., 2008. Rutile solubility in H2O, H2O-SiO2 and H2O-NaAlSi3O8 fluids at 0.7-2.0GPa and 700-100°C: Implications for solubility of nominally insoluble elements. Chem. Geol., 255, 1-2, 283-293.

Audetat A., Günther D., 1999. Mobility and H2O loss from fluid inclusions in natural quartz crystals. Contributions to Mineralogy and Petrology 137, 1-14.

Audetat A., Pettke T., 2006. Evolution of a porphyry-Cu mineralized magma system at Santa Rita, New Mexico (USA). Journal of Petrology 47, 10, 2021-2046.

Ballhaus C., Ryan C.G., Mernagh T.P., Green D.H., 1994. The partitioning of Fe, Ni, Cu, Pt, and Au between sulfide, metal, and fluid phases: A pilot study. Geochimica et Cosmochimica Acta, 58, 2, 811-826.

Becker S.P., 2008. Fluid inclusion characteristics in magmatic-hydrothermal ore deposits. PhD thesis, Virginia Polytechnic Inst. And State Univ., Blacksburg,VA, 138p.

Becker S.P., Fall A., Bodnar R.J., 2008. Synthetic Fluid Inclusions. XVII. PVTX Properties of high salinity H_2O-NaCl solutions (>30 wt % NaCl): application to fluid inclusions that homogenize by halite disappearance from porphyry Copper and other hydrothermal ore deposits. Economic Geology, 103, 539-554.

Berbeleac I., 1985. Gold Deposits (in romanian). Editura Tehnica. 334 p., Bucharest.

Berbeleac I., 1988. Ore deposits and global tectonics (in romanian). Editura Tehnica. 323p., Bucharest.

Berbeleac I., Popa T., Ioan M., Iliescu D., Costea C., 1995. Main characteristics of Neogene volcanic - subvolcanic structures and hosted deposits in Metaliferi Mountains. Geologica Macedonica, 9, 51-60.

Bodnar R.J., Burnham C.W., and Sterner S.M., 1985. Synthetic fluid inclusions in natural quartz. III. Determination of phase equilibrium propertiesin the system H2O-NaCl to 1000°C and 1500 bars: Geochimica et Cosmochimica Acta, 49, 1861-1873.

Bodnar R.J., 1995. Fluid-inclusion evidence for a magmatic source for metals in porphyry copper deposits.In Magmas, Fluids, and Ore deposits, Thompson J.F.H. (ed), Mineralogical Association of Canada, Short Course Series, 23, 139-152.

Bodnar R.J., 2003. Reequilibration of fluid inclusions. In I. Samson, A.Anderson, and D. Marshall, eds. Fluid Inclusions: Analysis and interpretation. Mineralogical Association of Canada, Short Course 32, 213-230.

Bodnar R.J., 2010. Magmatic fluid evolution associated with epizonal silicic plutons. ACROFI – III and TBG- XIV Abstr.Vol., Novosibirsk, Russia, 30-31.

Boştinescu S., 1984. Porphyry copper systems in the south Apuseni Mountains- Romania. Anuarul Institutului Geologic al Romaniei, LXIV, 163-174.

Burnham C.W., 1979. Magmas and hydrothermal fluids. In: Barnes H.L.(ed.) Geochemistry of Hydrothermal Ore Deposits. John Wiley & Sons, New York, 2, 71- 136.

Burnham CW, Ohmoto H., 1980. Late-stage processes of felsic magmatism. Mining Geology Special Issue 8:1-11.

Campos E., Touret J.L.R., Nikogosian I., Delgado J., 2002. Overheated, Cu-bearing magmas in the Zaldivar porphyry-Cu deposit, Northern Chile. Geodynamic consequences.Tectonophysics, 345, 229-251.

Cathles L.M., Shanon R., 2007. How potassium silicate alteration suggests the formation of porphyry ore deposits begins with the nearly explosive but barren expulsion of large volumes of magmatic water.Earth and Planetary Science Letters, 262, 92-108.

Cioacă M.E., 2011. Fluid evolution in the Bolcana ore deposit, Metaliferi Mountains (Romania). Carpathian Journal of Earth and Environmental Sciences, 6, 215-224.

Cline J.S., Bodnar R.J., 1991. Can economic porphyry copper mineralization be generated by a typical calc - alkaline melt ?. Journal of Geophysical Research, 96, 8113-8126.

Cline J. S., Bodnar R.J., 1994. Direct evolution of a brine from a crystallizing silicic melt

at the Questa, New Mexico, molybdenum deposit. Economic Geology, 89, 1780-1802.

Clocchiatti R., 1975. Les inclusions vitreuses des crystaux de quartz. Memoirs Soc. Geol., Fr. 122, 96 p.

Cloke P.L., Kesler S.E., 1979. The halite trend in hydrothermal solutions Economic Geology, 74, 1823-1831.

Cloos M., 2001. Bubbling magma chambers, cupolas, and porphyry copper deposits: International Geol. Rev., v. 43, p. 285-311.

Cună S., Palibroda N., Cună C., Pintea I. (2001) The mass spectrometric method for analysis of volatile species from fluid inclusions. Romanian Journ of Min. Dep. Vol 79 Suppl.2.ABCD-GEODE, 2001 workshop Vata Bai, Romania Abstr. Vol., 48-49.

Damman A.H., Karis S.M., Touret J.L.R., Rieffe E. C., Kramer J.A.L.M., Vis R.D., Pintea I., 1996. PIXE and SEM analysis of fluid inclusions in quartz crystals from the K-alteration zone of the Roşia Poieni porphyry-Cu deposit, Apuseni Mountains, Rumania. Eur. J. Mineral. 8, 1081-1096. Stuttgart.

Davidson P., Kamenetsky V.S., 2007. Primary aqueous fluids in rhyolite magmas: melt inclusion evidence for pre-and post-trapping exsolution. Chemical Geol., 237, 372-383.

Doglioni C., Tonarini S., Innocenti F., 2009. Mantle wedge asymmetries and geochemical signatures along W-and E-NE- directed subduction zones. Lithos, 113, (1-2), 179-189.

Driesner, T., Heinrich, C., 2007. The system H_2O-NaCl. Part I: Correlation formulae for phase relations in temperature-pressure-composition space from 0 to 1000°C, 0 to 5000 bar, and 0 to 1 X_{NaCl} . Geochimica et Cosmochimica Acta, 71, 4880-4901.

Eastoe C.J., Eadington P.J., 1986. High - temperature fluid inclusions and the role of the biotite granodiorite in mineralization at the Panguna porphyry copper deposit, Bougainville, Papua New Guinea. Economic Geology, 81, 478-483.

Eugster H.P., 1986. Mineral in hot water. Amer. Mineralogist, 71,.655-673.

Frezzotti M.L., 1992. Magmatic immiscibility and fluid phase evolution in the Mount Genis granite (southeastern Sardinia, Italy). Geochimica et Cosmochimica Acta, 56, 21-33.

Fulignati P., Kamenetski V.S., Marianelli P., Sbrana A., A., Mernagh T.P., 2001. Melt inclusion record of immiscibility between silicate, hydrosaline and carbonate melts : Applications to skarn genesis at Mount Vesuvius. Geology, 29, 11, 1043-1046.

Fulignati P., Kamenetski V.S., Marianelli P., Sbrana A., 2005. Fluid inclusion evidence of second immiscibility within magmatic fluids (79 AD eruption of Mt Vesuviu).Per. Mineral.74, 1, 43-54.

Ghiţulescu T.P., Socolescu M., 1941. Etude geologique et miniere des Monts Metaliferes. Anuarul Institutului Geologic al României, XXI, 284 p. Bucharest.

Grancea L., Cuney M., Leroy J.L., 2001. Mineralised versus barren intrusions: a melt inclusion study in Romania's Gold Quadrilateral.Comptes Rendus Academie de Sciences, Paris, Sciences de la Terre et des planetes/Earth and Planetary Sciences, 333, 705-710.

Hall D.L., Sterner M.S., 1993. Preferential water loss from synthetic fluid inclusions. Contributions to Mineralogy and Petrology, 114, 489-500.

Halter W.E., Heinrich C.A., Pettke T., 2005. Magma evolution and the formation of porphyry Cu-Au ore fluids: evidence from silicate and sulfide melt inclusions. Mineral Deposita 39, 845-863.

Harris C., 1986. A quantitative study of magmatic inclusions in the plutonic ejecta of Ascension Island. J. Petrol. 27 (1), 257-276.

Harris C.A., Golding S.D., 2002. New evidence of magmatic - fluid - related phyllic alteration: implications for the genesis of porphyry Cu deposits.Geology, 30, 4, 335-338.

Harris C.A., Kamenetsky V. S., White N. C., van Achterbergh E. and Ryan, C. G., 2003. Silicate-melt inclusions in quartz veins: Linking magmas and porphyry Cu deposits. Science, 302, 2109-2111.

Harris C.A., Kamenetsky V.S.,White N.C., Steele D.A., 2004. Volatile phase separation in silicate magmas at Bajo de la Alumbrera porphyry Cu-Au deposit, NW Argentina. Res. geol., 54, 3, 341-356.

Harris C.R., Pettke T., Heinrich C.A., Roşu E., Woodland S., Fry B., 2013. Tethyan

mantle metasomatism creates subduction geochemical signatures in non-arc Cu-Au-Te mineralizing magma, Apuseni Mountains (Romania). Earth and Planetary Science Letters, 366, 122-136.

Hattori K.H., Keith J.D., 2001. Contribution of mafic melt to porphyry copper mineralization: evidence from Mount Pinatubo, Philippines, and Bingham Canyon, Utah, USA. Mineral Dep. 36, 799-806.

Heinrich C.A., Halter W., Landtwing M.R., Pettke T., 2005. The formation of economic porphyry copper (-gold) deposits: constraints from microanalysis of fluid and melt inclusions. In: Mineral Deposits and Earth Evolution (eds Mcdonald I., Boyce A.J., Butler I.B., Herrington R.J., Polya D.A.), Geological Society Special Publication, London, Vol. 248, 247-63.

Heinrich C.A., 2007. Fluid-fluid interactions in magmatic-hydrothermal ore formation: Reviews in Mineralogy and Geochemis¬try, 65, 363-387.

Ianovici V., Vlad S., Borcoş M., Boştinescu S., 1977. Alpine porphyry copper mineralization of west Romania. Mineral. Deposita 12, 307-317.

Ivăşcanu P.M., Pettke T., Kouzmanov K., Heinrich C.A., Pintea I., Rosu E., Udubaşa G., 2003. The magmatic to hydrothermal transition: Miocene Deva porphyry copper - gold deposit, South Apuseni Mts, Romania. In Proc.7th Biennial SGA "Mineral Exploration and Sustainable Development" (Eliopoulos et al., eds), Athens, 24-28.

Kamenetsky V.S., Naumov V.B., Davidson P., van Achterbergh E.V., Ryan C.G., 2004. Immiscibility between silicate magmas and aqueous fluids: Amelt inclusion pursuit into the magmatic-hydrothermal transition in the Omsukchan Granite (NE Russia): Chemical Geology, v. 210, 73-90.

Kamenetsky V.S., Danyushevsky L.V., 2005. Metals in quartz-hosted melt inclusions: natural facts and experimental artifacts. Amer. Mineral. 90, 1674-1678.

Kamenetsky V.S., 2006. Melt inclusion record of magmatic immiscibility in crustal and mantle magmas. In Min. Assoc. of Canada, Short Course Series 36, 81-98, Montreal, Quebec.

Kamenetsky V.S., Kamenetsky M.B., 2010. Magmatic fluids immiscible with silicate melts: examples from inclusions in phenocrysts and glasses, and implications for magma evolution and metal transport. Geofluids, 10, 293-311.

Keith J.D., Whitney J.A., Hattori K., Ballantyne G.H., Christiansen E.H., Barr D.L., Cannan T.M., Hook C.J., 1997. The role of magmatic sulfides and mafic alkaline magmas in the Bingham and Tintic mining districts, Utah. Journal of Petrology, 38, 1679-1690.

Koděra P., Bakos F., Lexa J., Heinrich C.A., Wälle M., Falick A.E., 2012. Au-porphyry systems in Western Carpathians-mineralization, alteration patterns, and outstanding fluid properties.European Mineralogical Conference vol 1., EMC 2012-667.

Koděra P., Heinrich C.A. Wälle M., Lexa J., 2014. Magmatic salt melt and vapor:extreme fluids forming porphyry gold deposits in shallow subvolcanic settings. Geology, published online 10 April 2014.

Koster van Groos A.F.K., Wyllie P.J., 1969. Melting relationships in the system $NaAlSi_3O_8$-NaCl-H_2O at one kilobar pressure, with petrological applications. Journal of Geology, 77, 581-605.

Kouzmanov, K., Ivascanu, P., O'Connor, G., 2005. Porphyry Cu-Au and epithermal Au-Ag deposits in the southern Apuseni Mountains, Romania - South Apuseni Mountains district: Lat. 46 degrees 03' N, Long. 22 degrees 58'E. Ore Geology Reviews, 27, 46-47.

Kouzmanov, K., von Quadt, A., Heinrich, C.A., Pettke,T., Rosu, E., 2006. Geochemical and time constraints on porphyry ore formation in the Barza magmatic complex, Apuseni Mountains, Romania. - IGCP Project 486 - Proceedings of the 2006 Field Workshop, Izmir, Turkey, 24-29 Sept. 2006.

Kouzmanov, K., Pettke, T., Heinrich, C.A., 2010. Direct analysis of ore-precipitating fluids: combined IR microscopy and LA-ICP-MS study of fluid inclusions in opaque ore minerals. Economic Geology, 105, 351-373.

Kovacs M., 2002. Subduction-magmatic rocks petrogenesis in the Central- SE- zone from

Gutâi Mountains., Ed, Dacia, Cluj-Napoca, 201 p (in Romanian).

Landtwing M.R., Pettke T., Halter E.W., Heinrich C.A., Redmond P.B., Einaudi M.T., Kunze K., 2005. Copper deposition during quartz dissolution by cooling magmatic-hydrothermal fluids: The Bingham porphyry.Earth and Planetary Science Letters, 235, 229-243.

Larocque, A. C. L., Stimac, J. A., Keith, J. D., Huminicki, M. A. E., 2000. Evidence for open-system behavior in immiscible Fe-S-O liquids in silicate magmas; implications for contributions of metals and sulfur to ore-forming fields.Canadian Mineralogist, 38, 1233-1250.

Lerchbaumer L., Audetat A., 2012. High Cu concentrations in vapor-type fluid inclusions: an artifact?.Geochimica et Cosmochimica Acta, 88, 255-274.

Li Y., Audetat A., Lerchbaumer L., Xiong L., 2009. Rapid Na, Cu exchange between synthetic fluid inclusions and external aqueous solutions: evidence from LA-ICP-MS analysis. Geofluids, 9, 321-329.

Li X.J., Li G.M., Qin K.Z., Xiao B., 2011. High temperature magmatic fluid exsolved from magma at the Duobuza porphyry copper - gold deposit, Northen Tibet.Geofluid, 11, 134-143.

Lowenstern J.B., 1994. Chlorine, fluid immiscibility and degassing in peralkaline magmas from Pantelleria, Italy. American Mineralogist, 79, 353 - 369.

Martel C., Bureau H., 2001. In situ high-pressure and high –temperature bubble growth in silicic melts.Earth and Planetary Science Letters, 191, 115-127.

Mavrogenes J.A., Bodnar R.J., 1994. Hydrogen movement into and out of fluid inclusions in quartz: Experimental evidence and geologic implications. Geochimica et Cosmochimica Acta, 58, 141 – 148.

Mârza I., 1999. Magmatic ore genesis. 4. Hydrothermal Metallogeny. Univ Press Cluj-Napoca, 485p (in Romanian).

Milu V., Leroy J.L., Piantone P., 2003. The Bolcana Cu-Au ore deposit (Metaliferi Mountains, Romania): first data on the alteration and related mineralization. C. R. Geosciences, 335, 671-680.

Milu, V., Milesi, J.P., and Leroy, J.L., 2004. Roşia Poieni copper deposit Apuseni Mountains, Romania: Advanced argillic overprint of a porphyry system: Mineraium. Deposita, 39, 173-188.

Mitchell A.H.G., Carlile J.C., 1994. Mineralization, antiforms and crustal extension in andesitic arcs. Geological Magazine, 131, 231-242.

Metrich N., Rutherford M.J., 1992. Experimental study of chlorine behavior in hydrous silicic melts. Geochimica et Cosmochimica Acta., 56, 607 – 616.

Muntean, J.L., and Einaudi, M.T., 2000. Porphyry gold deposits of the Refugio district, Maricunga belt, northern Chile: Economic Geology, 95, 1445-1472.

Nadeau O., Williams-Jones E., Stix J., 2010. Sulphide magma as a source of metals in arc-related magmatic hydrothermal ore fluids. Nature Geosciences, 3, 501-505.

Naumov V.B., Tolstykh M.L., Kovalenker V.A., Kononkova N.N., 1996. Fluid overpressure in andesite melts from Central Slovakia: Evidence from inclusions in Minerals. Petrology 4, 3, 265-276. Translated from Petrologiya 4, 3, 283-294.

Nedelcu, L., Roşu, E., Costea, C., 2003. Mineral microinclusions hosted in sulfides of main neogene porphyry copper and epithermal ore deposits of the south Apuseni Mountains, Romania. Acta Mineralogical-Petrographica. Abstr. Ser. 1, Szeged, 78.

Neubauer F., Lips A., Kouzmanov K., Lexa J., Ivăşcanu P., 2005.1: Subduction, salb detachment and mineralization: The neogene in the Apuseni Mountains and Carpathians.Ore Geology Reviews, 27, 13-44.

Pintea I., 1993. Microthermometry of the hydrosaline melt inclusions from copper-porphyry ore deposits (Apuseni Mountains, Romania). Arch. Mineral. XLIX, 165-167. Warsaw. Poland.

Pintea I., 1995. Fluid inclusion evidence for magmatic immiscibility between hydrous salt melt and silicate melt as primary source of ore metals in porphyry – copper system from Apuseni Mountains, Romania. Bol. Soc. Espagnola Mineralogia, 18-1, 184-186, Barcelona.

Pintea I., 1996. Fluid inclusion study, with special view on the fluid phase immiscibility associated to the neogene porphyry copper ore deposits genesis from Metaliferi Mountains (western Romania).

Unpublished Ph. D. Thesis. University of Bucharest, 172 p. (in Romanian).

Pintea I., 1997. The significance of the liquid homogenization temperature in salt melt inclusions. A case study in neogene porphyry copper ore deposits from Metaliferi Mountains (western Romania). ECROFI XIV, Nancy, Abstract Volume, 266-267. Nancy, France.

Pintea I., Udubaşa G., Nedelcu L., 1999a. Evolution of fluid phases related to a new porphyry copper deposit in Romania: The Ţibles massif. Mineral Deposits: Processes to processing, Stanley et al.(eds), 83-85, Balkema, Rotterdam.

Pintea I., Hopârtean E., Cosma V., Morar G.G., Hopartean I., Eggenkamp H.G.M.,1999b. Chloride content and chlorine stable isotope ratios of the salt melt inclusions from the Roşia Poieni porphyry copper ore deposit (Metaliferi Mountains, western Romania). ECROFI XV Abstracts, Terra nostra 99/6, 229-230 and Romanian Journal of Mineralogy, 79, Supplement no.1, 53. Bucharest.

Pintea I., 2001. Melt and fluid inclusions study in Neogene porphyry Cu-Au(Mo) from Metaliferi Mountains. Romanian Journal of Mineral Deposits, 79, suppl. 2, Field Guidebook, 28-30.

Pintea I., 2002. Occurrence and microthermometry of the globular sulfide melt inclusions from extrusive and intrusive volcanic rocks and related ore deposits from alpine Carpathian chain. Workshop-Short Course on Volcanic Systems Geochemical and Geophysical Monitoring. Melt Inclusions: methods, applications and problems.(B. De Vivo and R.J. Bodnar, Eds) Proceedings,177-180, September 26-30th, 2002-Grand Hotel Moon Valley, Seiano di Vico Equense (Sorrento Peninsula) - Napoli, Italy.

Pintea I., 2009. Still problematic facts on the fate of brines in the alpine porphyry copper systems in Romania. Procc. ECROFI XX, Granada (Spain), abstr. 187-188.

Pintea I., 2010. Fluid and melt inclusions evidences for autometasomatism and remelting in the alpine porphyry copper genesis from Romania. Romanian Journal of Mineral Deposits, 84, 15-18.

Pintea I., 2012. Fluid and melt inclusions: a precious tool in selective exploration strategy. Romanian Journal of Mineral Deposits, 85, 85-89.

Quan R.A., Cloke P.L., Kesler S.E., 1987. Chemical analyses of halite trend inclusions from Granisle porphyry copper deposit, British Columbia. Economic Geology, 82, 1912 - 1930.

Reyf F.G., Bazheyev Ye. D., 1977. Magmatogenic chloride solutions and tungsten mineralization. Geokhimia, 1, 63-70.

Reyf F.G., 1997. Direct evolution of W- rich brines from crystallizing melt within the Mariktikan granite pluton, west Transbaikalia. Mineralium Deposita, 32, 475-490.

Richards J.P., 2003. Tectono-magmatic precursors for porphyry Cu-(Mo-Au) deposit formation. Economic Geology, 98, 1500-1533.

Richards J.P., 2009. Postsubduction porphyry Cu-Au and epithermal Au deposits: Products of remelting of subduction-modified lithosphere. Geology, 37, 247-250.

Roedder E., Coombs D.S., 1967. Immiscibility in granitic melts, indicated by fluid inclusions in ejected granitic blocks from Ascension Island. Journal of Petrology, 8, 417-451.

Roedder E., 1970. Laboratory studies on inclusions in minerals of Ascension Island granitic blocks, and their petrologic significance. In : Yu . A. Kusnetsov (ed), Problems of Petrology and Genetic Mineralogy, V.S. Sobolev Memorial vol. II, "Nauka" Press Moscow, 247-258 (in russian translated in Fluid Inclusion Res., Proc.of COFFI, 5, 1972,129-138).

Roedder E., 1981. Natural occurences and significance of fluids indicating high pressure and temperature. In Chemistry and geochemistry of solutions at high temperature and pressures, Physics and chemistry of the earth, 13, (D.T. Rickard and F. E. Wickman, eds), Pergamon, 9-35.

Roedder E., 1984. Fluid Inclusions. Reviews in Mineralogy, 12, 644 pp., Mineralogical Society of America ,Washington.

Roedder E., 1992. Fluid inclusion evidence for immiscibility in magmatic differentiation.

Geochimica et Cosmochimica Acta, 56, 5-20.

Roşu E., Nedelcu L., Pintea I., Ivăşcanu M.P., Costea C., Şerban A., Alexe V., 2001. The estimation of the formation constraints of the main mineral deposit types. Romanian Journal of Mineral Deposits, 79, suppl. 2, Field Guidebook, 23-27.

Roşu E., Seghedi I., Downes H., Alderton D.H.M., Szakács A., Peckay Z., Panaiotu C., Panaiotu C.E., Nedelcu L., 2004. Extension-related Miocene calc-alkaline magmatism in the Apuseni Mountains, Romania: origin of magmas. Schwezerische Mineralogische und Petrographische Mitteilungen, 84, 153-172.

Ryabchikov I. D., 1963. Experimental study of the distribution of alkali elements between immiscible silicate and chloride melts. Dokl. Akad. Nauk SSSR, 14, 190-192.

Seedorff E., Dilles J.H., Proffett J.M., Einaudi M.T., Zurcher L., Stavast W.J.A., Johnson D.A., and Barton M.D., 2005. Porphyry deposits: Characteristics and origin of hypogene features., Economic Geology, 100th Anniversary Volume, 251-298.

Seghedi I., Downes H., Szakács A., Mason P.R.D., Thirlwall M.F., Rosu E., Pecskay Z., Marton E., Panaiotu C., 2004. Neogene-Quaternary magmatism and geodynamics in the Carpathian-Pannonian region: a synthesis. Lithos, 72, 117-146.

Seghedi I., Szakács A., Roşu E., Pecskay Z., Gmé lling K., 2010. Note on the evolution of a Miocene composite volcano in an extensional setting Zărand Basin (Apuseni Mts., Romania). Central European Journal of Geosciences, 2, 321-328.

Signorelli S., Carroll M.R., 2000. Solubility and fluid-melt partitioning of Cl in hydrous phonolitic melts. Geochimica et Cosmochimica Acta, 64, 2851-2862

Shahabpour J., 2000. Some sulphides-silicate assemblages from the Sar Cheshmeh porphyry copper deposit, Kerman, Iran. J. Sci. I. R. Iran, 11, 39-48.

Shinohara, H., Iiyama, J.T., Matsuo, S., 1989. Partition of chlorine compounds between silicate melt and hydrothermal solutions: I. Partition of NaCl-KCl. Geochimica et Cosmochimica Acta 53, 2617-2630.

Shinohara H., 1994. Exolution of immiscible vapor and liquid phases from a crystallizing silicate melt: implications for chlorine and metal transport. Geochimica et Cosmochimica Acta, 58, 5215-5221.

Shmulovich K.I., Mercury L., Thiéry R., Ramboz C., El Mekki M., 2009. Experimental superheating of water and aqueous solutions.Geochimica et Cosmochimica Acta, 73, 2457-2470.

Solovova I., Girnis A., Naumov V., Kovalenko V., Guzhova A., 1991. High-temperature heterogenity: evidences from microinclusions in Pantelleria volcanics. Plinius no. 5, ECROFI XI, abstr. vol., p. 206.

Stavast W. J. A.. Keith J. D., Christiansen E. H., Dorais M. J., Tingey D., Larocque, A., Evans N., 2006. The Fate of Magmatic Sulfides During Intrusion or Eruption, Bingham and Tintic Districts, Utah .Economic Geology,101, 329-345.

Thomas R., Webster J.D., Heinrich W., 2000. Melt inclusions in pegmatite quartz: complete miscibility between silicate melts and hydrous fluids at low pressure. Contributions to Mineralogy and Petrology, 139, 394-401.

Thomas R., Davidson P., 2012. Evidence of a water-rich silica gel state during the formation of a simple pegmatite. Mineralogical Magazine, 76, 2785-2801.

Udubaşa G., Edelştein O., Răduţ M., Pop N., Istvan D., Kovacs M., Pop V., Stan D., Bernad A., Götz A.,1983. The Ţibles neogene igneous complex of North Romania: Some petrologic and metallogenetic aspects.Anuarul Institutului Geologic al României, LXI, 285-295.

Udubaşa G., Rădut M., Edelştein O., Pop N., Istvan D., Pop V., Stan D., Kovacs M., Roman L., Bernad A., 1984. Metallogeny of the Ţibles eruptive complex, Eastern Carpathians. (in romanian). Dări de seamă ale şedinţelor Institutului Geologic al României, LXVIII , 221-241.

Udubaşa, G., Roşu, E., Seghedi, I. Ivăşcanu, P.M., 2001. The "Golden Quadrangle" in the Metaliferi Mts., Romania: what does this really mean? Romanian Journal of Mineral Deposits, 79, suppl. 2, 24-34.

Vasyukova O.V., Kamenetsky V.S. and Gömann K., 2008. Origin of “quartz eyes” and fluid inclusions in mineralized porphyries. Materials of reports of Goldschmidt Conference 2008 - “from Sea to Sky” July 13- 8 Vancouver, Canada, 955.

Vasyukova O., 2011. Types and origin of quartz and quartz hosted fluid inclusions in mineralized porphyries. PhD thesis, CODES, ARC, Centre of Excellence in ore deposits. Univ. of Tasmania, Australia, 213p.

Vlad S.N., 1983. Geology of porphyry copper deposits. Editura Academiei, 154 pp (in Romanian).

Vlad S.N., Orlandea E., 2004. Metallogeny of the gold quadrilateral: style and characteristics of epithermal-subvolcanic mineralized structures, south Apuseni Mts., Romania. Studia Univ. Babes-Bolyai, Geologia, XLIX , 2004, 15-31.

Veksler I.V., Thomas R., Schmidt C., 2002. Experimental evidence of three coexisting immiscible fluids in synthetic granitic pegmatite. Amer. Mineral., 87, 775-779.

Webster J.D., 1997a. Exsolution of magmatic volatile phases from Cl- enriched mineralizing granitic magmas and implications for ore metal transport. Geochimica et Cosmochimica Acta, 61, 1017-1029.

Webster J.D., 1997b. Chloride solubility in felsic melts and the role of chloride in magmatic degassing. Journal of Petrology, 38, 1793-1807.

Webster J.D., Mandeville C.W., 2007. Fluid immiscibility in volcanic environments. Rev. in Mineral. and Geochem.65, 313-362.

Wilkinson J.J., Nolan J., Rankin A.H.,1996. Silicothermal fluid: a novel medium for mass transport in the lithosphere.Geology, 24, 1059-1062.

Wilkinson L., Cooke D., 2011. Enhanced geochemical targeting in magmatic hydrothermal system. AMIRA P.1060.http://www.amira.com.au.

Williamson B.J., Wilkinson J.J., Luckham P.F., Stanley C.J., 2002. Formation of coagulated colloidal silica in high-temperature mineralizing mineralizing fluids. Mineralog. Mag. 66, 547-553.

Wilson J. W. J., Kesler S.E., Cloke P.L., Kelly W. C., 1980. Fluid inclusion geochemistry of the Granisle and Bell porphyry copper deposits, British Columbia., Economic Geology, 75,45-61.

Yang K., Bodnar R.J., 1994. Magmatic-hydrothermal evolution in the "Bottoms" of porphyry copper systems: evidence from silicate melt and aqueous fluid inclusions in granitoid intrusions in the Gyeongsang basin, South Korea. International Geol., Rev., 36, 608-628.